This is to certify that the

thesis entitled

IMPACT MEASUREMENT AND ANALYSIS SOFTWARE
FOR STUDYING APPLE DAMAGE

presented by

Brian Arnold Klug

has been accepted towards fulfillment
of the requirements for

M.S. degree in Agricultural Engineering

A. R. Zapp
Major professor

Date 6/30/87

IMPACT MEASUREMENT AND ANALYSIS SOFTWARE FOR STUDYING APPLE DAMAGE

By

Brian Arnold Klug

A THESIS

Submitted to
Michigan State University
in partial fulfillment of the requirements
for the degree of

MASTER OF SCIENCE

in

Agricultural Engineering

Department of Agricultural Engineering

1987

ABSTRACT

IMPACT MEASUREMENT AND ANALYSIS SOFTWARE
FOR STUDYING APPLE DAMAGE

By

BRIAN ARNOLD KLUG

A self-contained data acquisition unit about the size of an apple was developed to measure vector impacts (accelerations). The purpose of this data acquisition unit is to aid in the study of bruising to fruits and vegetables; particularly apples. The unit uses an Intel 8097 microcontroller to control data collection, data storage, and communications with appropriately designed software. A serial communication line is used to issue interactive commands and retrieve data. The data acquisition unit stores data for impacts above a predetermined threshold and formats the data into records consisting of triaxial acceleration values along with the time of occurrence. An impact analysis software package which runs on a personal computer was also developed. The analysis includes: peak acceleration, overall velocity change, impact duration and enhanced plots of the original impact data. Some trial results from an apple packing line are presented.

Approved:

H. Roland Zapp
Co-Major Professor

Bernie R. Tennes
Co-Major Professor

Donald M. Edwards
Department Chairman

ACKNOWLEDGEMENTS

The author wishes to express his sincere gratitude and appreciation to the following:

Dr. H. Roland Zapp, the author's co-major professor, for his help in developing the technical content of this thesis and for his many hours of reviewing and commenting on this manuscript.

Dr. Bernie R. Tennes, the author's co-major professor, for his guidance, support, and encouragement given during the development of the Instrumented Sphere.

John B. Gerrish, who served on the author's guidance committee, for his suggestions and comments.

Siamak Siyami, fellow graduate student, for his assistance and encouragement during this research.

The author also wishes to acknowledge the assistance and encouragement from the following graduate students: Henry A. Affeldt Jr., Paul Armstrong, and Bryan Murphy.

The author wishes to acknowledge that the following technical staff and undergraduate students helped accomplish this research effort: Joe R. Clemens, Sidney H. Ehlert, Richard J. Wolthuis, Chris Johnson, Robert Small, and Jim Kraft.

The author wishes to express his gratitude to Dr. Galen K. Brown and the United State Department of Agriculture for their support of this research.

TABLE OF CONTENTS

LIST OF TABLES

LIST OF FIGURES

LIST OF APPENDICES

1. Introduction

1.1 Research Relevance

Quality in fresh produce, such as apples, plays a major role in their demand to comsumers who expect picture-perfect fruit. Bartram (1977) indicated that bruising was a major cause of apple quality reduction, finding a maximum of 211 (12.7 mm diameter) bruises in 100 Red Delicious apples and 169 (12.7 mm diameter) bruises in 100 Golden Delicious apples sampled from retail outlets in March and April. Mattus (1980) also found bruising to be the most serious fault in fresh apples with 43.5% of the apples at distribution centers having at least one bruise greater than 12.7 mm in diameter.

Bruising can occur anywhere between the apple tree and the retail store shelves and varies with variety, picker, packing house and shipper. With this many variables it is difficult to correlate results from one bruise study to the next. The study of bruising could be made easier if the effects due to apple properties were separated from the effects due to handling equipment. Some of the interesting handling equipment effects include: peak deceleration, impact duration, overall velocity change, impact velocity, impact surface properties and the number of impacts experienced.

The effects from handling equipment can be separated from the effects related to apple properties by developing a pseudo-fruit which contains an impact sensor and has physical properties which remain constant from test to test. The development of such a pseudo-fruit has received the attention of many researchers.

The pseudo-fruit, developed by others had technical problems and limitations, prompting the research described in this thesis. A pseudo-fruit, first described by Tennes et al. (1986), has been developed which is microcontroller-based, battery powered and uses random access memory (RAM) for data storage. In order to implement the pseudo-fruit, an operating system and data collection software had to be developed as described in chapter 2.

By studying the impact data (triaxial acceleration values) recorded from the pseudo-fruit, problem areas in the handling of apples and other agricultural commodities can be readily identified so that corrective actions may be taken. The analysis techniques and software decribed in chapter 3 were developed to study the impact data. Using the pseudo fruit, any handling system changes added for bruise reduction can also be checked for effectiveness.

1.2 Objectives of the Research

The major research objectives can be briefly stated as follows:

1. Develop a real-time operating system and serial communication program for a miniature microcontroller-based impact measurement device (Instrumented Sphere or IS).
2. Develop a sampling routine for the Instrumented Sphere which can sample 3 accelerometers at 1000 hz or faster and based on a threshold value conditional store the data in Random Access Memory (RAM).
3. Develop software and techniques to analyze the impact (acceleration) data.

1.3 Previous Impact Detection Devices

A number of Impact Detection Devices (pseudo-fruit) have been proposed and fabricated for the purpose of investigating the causes of damage to agricultural products due to impact and shock. Part of the technology used in these Impact Detection devices has come from other engineering applications. Harrison (1968) had already been working on devices to measure acceleration under impact conditions for non-agricultural objects before O'Brien et al. (1973) described their first Pseudo-Fruit in 1973 (work had started in 1970). Both the Harrison and O'Brien devices employed telemetry where the signal was transferred by radio to a data storage device. Another innovation of O'Brien et al. was the use of a tri-axial accelerometer instead of using a single axis accelerometer which had been used by previous agricultural researchers with connected cables.

In the O'Brien device, the electronics and sensor were housed in a 50.8 mm (2 in) diameter hollow fiberglass sphere covered by a 10.2 mm (0.4 in) thick layer of resilient material. The goal of O'Brien et al. was to make the pseudo-fruit with physical properties resembling those of actual fruit so

that the acceleration (or force) measured could be directly correlated with that of fruit. The pseudo-fruit contained three miniature FM transmitters with antennas, one for each axis. A standard FM receiver, with the "de-emphasis" circuit eliminated, was used to pick up the pseudo-fruit signal. A multi-channel analog tape recorder was then used to record the telemetry signals along with a timing signal. Due to low transmitter power, the receiver's antenna had to be placed very close to the pseudo-fruit; thus the system had a major limitation.

The pseudo-fruit of O'Brien et al. could measure accelerations as low as 0.5 g with an estimated accuracy of ±5 percent and a frequency response down to 2 Hz. They did admit that more calibration work was required.

In conjunction with the work of O'Brien et al., Rider et al. (1973) studied the pseudo-fruit's calibration and how it would correlate to bruise damage in fruit. Since previous work by other researchers had indicated that bruising is caused by excessive internal shear stress, Rider calibrated the accelerometer outputs to the shear stress experienced by the pseudo-fruit. Thus the shear stresses experienced by the pseudo-fruit were supposed to correlate directly to bruise damage. All of Rider's formulas assumed perfectly elastic impacts. In order to test the mathematical relationships, a 76.2 mm (3.0 in) diameter pseudo-fruit containing a piezoelectric triaxial accelerometer was constructed. This encased sensor was connected to a tape recorder by a flexible cable. The shell of the pseudo-fruit was a 1.52 mm (0.06 in) thick 57.15 mm (2.25 in) diameter steel sphere covered with a layer of 9.53 mm (3/8 in) thick type AH Ensolite^{R} over which three layers of 3M* Fastbond-10^{R} contact cement were applied. The accelerometer was rigidly mounted inside the shell. The unit had a weight of 204 gm (0.45 lb) and a coefficient of restitution of 0.42 when dropped 152.4 mm (6 in) onto concrete. The modulus of elasticity of the pseudo-fruit, 489 kPa (71 psi), was determined both by measuring the area of contact during impact and by using a quasi-static compression test. In Rider's calibration procedure the only externally supplied variable, was the modulus of elasticity of the impacted surface. From the impact data, he only

*Mention of a product or company name does not constitute an endorsement of the product or company by the author or Michigan State University. Trade names are used solely to provide specific information.

made use of the peak acceleration and impact duration. In order to make the theoretical calibration procedure correspond to experimental data however, the impact duration time had to be multiplied by a unexplained factor of 2 before being used in the calibration procedure.

Aldred and Burch (1977) added a microcomputer to their impact detection system and an analog vector summing circuit. Their impact detection system consisted of a sensing unit and receiving station. Instead of transmitting 3 channels of data, only one channel was transmitted. The FM tuner used to receive the signal, utilized a 10 kHz subcarrier which was converted to 1.28 MHz by a phase-locked loop. An 8-bit counter was used to count the zero transitions which are proportional to the acceleration amplitude during the sample period. Aldred and Burch used a sampling rate of 1000 Hz which allowed for only 2 seconds worth of data storage in memory. In order to plot the data, it was converted back to analog so that a strip chart recorder could be used. The actual sensing unit consisted of four 57.2 mm diameter circuit boards bolted together with spacers between them. The whole unit was housed in a 66.6 mm acrylic sphere with a total weight of 86 gm. The sensor unit could operate for three hours on two 7-volt batteries used for power. For storage, the sensor unit had a magnetic switch to turn the power off and on.

Among the electronic impact detection devices, was a mechanical impact detection device developed by Jenkins and Humphries (1982) using fluid filled bladders with slit valves to meter fluid flow during impacts. The bladder used was actually a 76 mm toy basketball fitted with six equally spaced pharmaceutical slit valves. Before each test, the bladder was filled with water and weighed. After the test was complete, the bladder was weighed again, and the water loss was found to be proportional to the impact velocity. These impact tests were repeated and the statistical averages used to make conclusions about various sweet potato handling techniques. The problem with the method was the lack of an automated recording system.

Anderson and Parks (1984) developed two impact detection devices (two physical units) using a pressure sensor transducer in one and single axis accelerometer in the other. Both devices used telemetry to transmit data to a receiver with attached tape recorder. A two channel tape recorder was

used so that data could be recorded on one channel and voice commentary on the other. Both devices used the same FM transmitter design and battery configuration which could operate for eight hours. A jack socket was used to recharge the batteries and provide an off/on switch. For the pressure transducer version, a miniature piezoresistive sensor was placed inside a sealed 60 mm diameter rubber ball. The transmitter, batteries and jack were cemented to the outside of the rubber ball using silicone rubber. The package was completed by sealing the entire package with a self-amalgamating rubber tape, thereby producing a tuber-shaped device. The accelerometer version was assembled by first attaching the accelerometer, the radio capsule, the batteries and the jack socket to a 44 mm by 34 mm platform. The platform was sandwiched between two layers of 25 mm thick high density foam before being wrapped in self-amalgamating rubber tape. The pressure version was calibrated by compressing it between two plates with a known force, while the accelerometer version was calibrated by dropping it from known heights. The acceleration data was used to generate an "equivalent drop height number". These devices were used to test potato handling equipment.

By 1983, Halderson et al. (1983) were developing their first generation impact detection device based on telemetry and using triaxial accelerometers. Their first unit consisted of an accelerometer, attenuation circuit, 2.7 volt battery, three transmitters and a dipole antenna. This unit was enclosed by a hardwood body covered with molded rubber strips bonded together with a plasticized surface coating. The two halves of the enclosure were held together with two metal screws. However the transmitted signal was unacceptably directional.

Halderson's second generation impact detection device used a single transmitter system with three subcarriers. A Columbia model 612-TX triaxial piezoelectric accelerometer was used which could sense up to 1000 g at frequencies between 2 and 5000 Hz The antenna for the unit consisted of two loops oriented 90 degrees to each other, which proved to be less directional. A special three channel FM telemetry receiver was used to receive the transmitted signal. During impact tests, the enclosed accelerometer voltage correlated slightly better than 80% wit' the FM receiver's output. Range tests

showed that the unit had a range of approximately 30 meters. More calibration tests however were required at the time of publishing.

By 1986, Halderson et al. (1986) had built and tested a third generation impact detection device. The main changes from his previous device were in the packaging. The new unit enclosed all of the electronics in a 40 mm X 40 mm X 57 mm aluminum box. Three small LC antennas were mounted on the outside of the three perpendicular planes of the box. The aluminum box was molded in silicone (Dow Corning RTV-3110) to form a cylindrical package that was 100 mm in length and 84 mm in diameter, weighed 654 gm, and had an overall specific gravity of 1.18. The device was tested under impact conditions by dropping a 286.7 gm metal rod, with a spherical hard rubber tip (365 mm in dia.), onto the device which was supported by a 75 mm thick foam pad with a force-deflection rate of $275(g/cm^2)/cm$. During the tests the rod was dropped from a height such that it would have 0.2J of kinetic energy upon impact. Ten replications were made for each of the three axes producing coefficients of variation of 8.3%, 8.4% and 5.2% respectively for the X, Y and Z axes. The transmission distance was evaluated around a potato harvester, but no range distances were reported.

Siyami et al. (1986) described the hardware for a NMOS microcontroller-based impact detection device with an external triaxial accelerometer connected via cable to the microcontroller box. This unit was battery powered, had 48 Kbytes of RAM, 8 Kbytes of Erasable Programmable Read Only Memory (EPROM) and used an Intel 8097 microcontroller with an on-board analog to digital converter. The Software for this unit was described by Klug et al. (1986).

The hardware described in this thesis will be a refined version of Siyami's hardware and will contain an internal accelerometer with all of the hardware being embodied in a 140 mm diameter epoxy sphere.

2. Data Acquisition Unit

2.1 Previous Digital-based Data Acquisition Units

The application of digital electronics to data acquisition systems (some of which are also miniature) has been common. A miniature cardiotachometer, which was developed by Zsombor-Murray et al. (1981), is an example of such a digital-based data acquisition unit. A cardiotachometer counts heart beats over a short time interval (10 seconds) using the EKG signal as input. Zsombor-Murray's cardiotachometer was the size of a cigarette pack and weighed less than 500 g with battery and contained 1 Kbyte of RAM. The analog EKG signal was amplified, filtered and converted to square pulses before being sent to a digital counter which was sampled every 10 s. The cardiotachometer did not utilize a microprocessor but handled data collection and retrieval through hard wired logic. Data retrieval was handled through a special TTL parallel interface.

Ball Systems Division (1985) described a miniature self-contained temperature recording device in a preliminary product data sheet which was microprocessor-based. The miniature 54.6 mm by 35.1 mm diameter cylindrical dimensions of Ball's device were obtained by the integration of a microcomputer on a hybrid substrate. The main drawbacks of using this system to measure impacts are: the system has only one channel, can store only 1000 samples, and was customized to record temperature only.

Ahrens and Searcy (1985) developed a larger multi-channel microcontroller-based data acquisition unit for logging the activity of cattle on the range which was small enough to be carried by cattle without bothering them. Their system was based on CMOS technology with the heart being an Intel 80C31, which is an 8-bit microcontroller with 128 bytes of on-board RAM, three 8-bit addressable I/O ports, two 16-bit timer/counters, a full duplex serial port and the capability of directly supporting 64K each of external program memory and data memory. Program memory consisted of 4 Kbyte of EPROM and 2 Kbyte of EEPROM while the data memory could consist of up to 32 Kbytes of RAM depending

on the configuration. The system also contained an 8-bit, 8 channel A/D converter and a real time clock which made chronological logging possible since the unit could be logging for several days without intervention. Both the hardware and software were modular in design with the hardware boards being functional blocks (memory or sensors) and the software modules being functional routines called from an executive program. The chewing and walking habits of the cattle were of primary interest to the researchers. Significant motion from these habits produced 5 volt pulses out of the sensor and conditioning circuits which could be sent to the microcontroller. Besides the data collection software, the software also contains a complete monitor which could be used by connecting a terminal to the serial port. Despite being portable, this unit was still much larger than an apple.

Digital data acquisition also makes it practical to sample transducers continuously but store data only when a threshold is exceeded, which is what Adam et al. (1985) did with his telemetric seismic data-acquisition system. Adam's system consisted of remote encoding stations and data acquisition substations. Each remote encoding station consisted of up to three seismic sensors, filters, an analog to digital converter (μ-255 companding law CODEC), a timing circuit and a digital UHF FM transmitter. The μ-255 companding law CODEC uses a non-linear coding technique similar to the IEEE floating point convention to code the A/D result. These remote encoding units sampled continuously at 60 samples/s per channel. The data-acquisition substations consisted of UHF receivers, demodulators, and a digital data processing facility implemented by a multi-microprocessor system. The main microprocessor handled serial input from the possible 24 radio receivers and threshold detection while the slave microprocessor handled modem communications to a data analysis center and possible tape storage. Each substation had enough memory to hold up to 20 seconds of data which could include pre-threshold data if desired. From the 8-bit CODEC data byte, only 4 of the bits were used in the threshold detection algorithm. The algorithm consisted of dividing the short term average magnitude by the long term average magnitude and comparing it to a threshold value. If any of the possible 24 encoder stations registered above the threshold for a predetermined time, all of the encoder stations are recorded. Recording terminates when all of the signals are below the threshold for a short period of time. The process of dividing the short

term average by the long term average makes the thresholding process immune to nonseismic disturbances such as rain and eliminates the need for threshold adjustments.

With a digital data acquisition system, it is possible to do more data processing then just threshold checking. Hill and Alderson (1981) developed a microprocessor-based digital wattmeter which incorporated variable sampling rates and numerical integration. Variable sampling rates are needed since the frequency of the input wave is an unknown and the numerical integration to get power must cover one period of the input wave and contain a sufficient number of samples (30). The digital part of the wattmeter was based on the Motorola M6800 microprocessor and contained 2 Kbyte of PROM, 256 bytes of RAM and a 12-bit A/D converter. The microprocessor was informed of input signal zero crossings through an interrupt generating circuit. The period of the input wave was determined by using a program counter loop to count the number of loops between two consecutive interrupts. The counter value then was used to calculate the sampling rate; data sampling was implemented by a program loop with padding instructions. After sampling for one period of the input wave, the average watts are calculated and displayed. The software requires, at minimum, 4 periods of the input wave to update the display.

Sridharan (1984) recognized problems with time multiplexed A/D converter data acquisition systems and developed a synchronous multichannel data acquisition system by using a separate A/D converter for each channel. All of the result registers for the A/D converters were addressed through the memory map. The "go" bit on the A/D converters was addressed through a common memory address which caused all of the conversions to start at the same time. When implemented on a SDK-85 single board computer, Sridharan was able to convert and store the results of 8 channels with the use of only 93 μs of CPU time.

Wallingford (1982) also did some clever interfacing of A/D converters to microprocessors to boost the performance of his data acquisition system. Wallingford's data acquisition system was implemented on a 16-bit TI9900 microcomputer and also used memory map addressable A/D converters. The key to Wallingford's system was the way he used bus signals generated by the indirect auto-increment

MOV instruction. The read portion of the instruction reads the A/D results and resets the converters for the next conversion while the write portion of the instruction starts the next conversion and stores the previous results to memory. With Wallingford's system, only one instruction is required per sample point. The only interfacing hardware needed is an address decoder and RS flipflop. Wallingford was able to convert two 8-bit channels at 115 kHz. in parallel since the TI9900 is a 16-bit processor. Unfortunately Wallingford's and Sridharan's systems used more hardware than what would fit in an apple sized impact measurement device.

Barnes et al. (1978) applied finite-state models to the development of data acquisition software in order to improve reliability and simplify debugging. The goal of Barnes's research was to improve the efficiency of cotton gins by measuring such parameters as bale weight, electric power, gas consumption, temperature, humidity and gin component positions throughout the day. The data from the discrete inputs, TTL inputs and analog inputs were recorded on cassette tape by the data acquisition unit (DAU) and later sent to a processing center for analysis. The software was an infinite loop containing the following modules: Time Monitor, Keyboard Monitor, Display Monitor, A/D Monitor, Tape Monitor and State Control. Even though the last module in the loop was dedicated to state control, all of the modules made use of the 4-bit state variable for decision making. Since the DAU was centered around a cassette recorder, most of the finite-state model was related to the tape recorder. The state variable could be changed by switches on the keyboard, sampling rate timers and the tape position. The data on the cassette tape was formatted in blocks.

Higuchi et al. (1977) directed their efforts at improving the user friendliness of microprocessor-based signal processors by recognizing that not everyone using a microprocessor-based signal processor wanted to learn and use assembly language to program the processor. Therefore Higuchi created a block diagram signal processing "macro language" which used an interpreter located in ROM to carry out the instructions in real time. Higuchi's system was based on a NEC μCOM-4 microprocessor and had the following peripherals: 1024 bytes of ROM, 768 bytes of RAM five I/O ports, serial pipeline multiplier,

A/D converter and D/A converter. The overhead of using the interpreter reduced the maximum sampling rate for a second order filter to 59 samples/s.

2.2 Instrumented Sphere Hardware

The electronic hardware for the IS consists of two circuit boards (analog and digital), triaxial accelerometer, batteries and a five pin connector to the outside world. The digital circuit board contains the microcontroller, a crystal, address latches, and two RAM chips. The analog circuit board contains the voltage regulators, constant current sources, and three integrated amplifying and filtering chips. The five pin connector contains pins for serial communications, recharging, and shut down. Figure 2.1 shows a diagram of the IS electronic hardware.

2.2.1 Microcontroller

The digital board is designed around an Intel 8097 (A8797BH) NMOS 16-bit microcontroller which contains an internal serial port, timers and an Analog to Digital (A/D) converter (Figure 2.2). The 8097 is a register-based processor, containing 256 internal 8-bit registers which can also be joined together and used as 16-bit registers. Besides the 256 registers, this version of the 8097 also contains 8

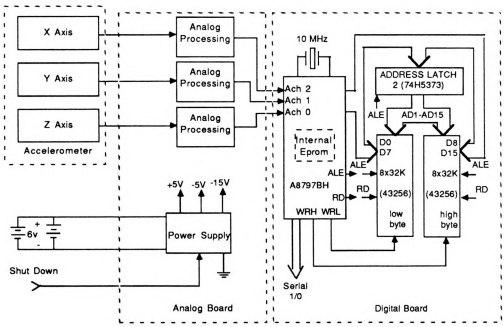

Figure 2.1. Block diagram of the IS hardware.

kbyte of Erasable Programmable Read Only Memory (EPROM) which can be used for program storage. This EPROM is programmed by using a special EPROM burner.

The A8797BH version of the 8097 microcontroller comes in a 68 pin grid array package (Figure 2.3) and is capable of physically addressing 64 kbytes of memory . This version of the 8097 provides control lines for the odd and even banks of memory. The IS uses a 10 MHz crystal with this version of the 8097.

The A8797BH version of the 8097 microcontroller contains a multiplexed 8 channel 10-bit A/D converter with sample and hold. The input range for the A/D converter is between 0V and 5V; therefore the accelerometer voltage has to be offset in order to have both positive and negative signals. The A/D conversion is done by successive approximation and requires a fixed time of 264 crystal cycles (or 26.4 μs with a 10 MHz crystal).

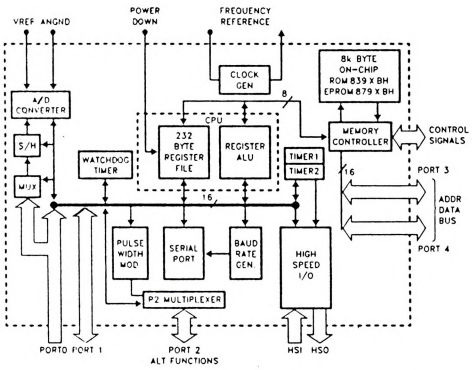

Figure 2.2. Block diagram of the A8797BH Microcontroller (Intel Corporation, 1986.).

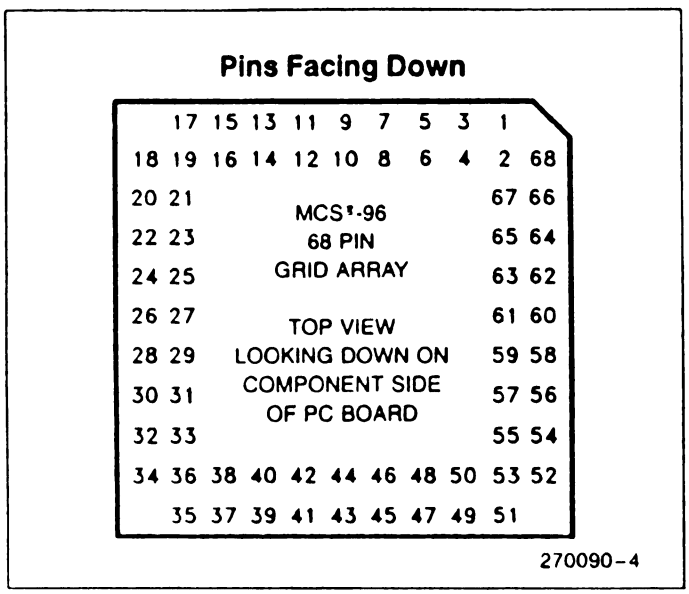

PGA/ LCC	PLCC	Description	PGA/ LCC	PLCC	Description	PGA/ LCC	PLCC	Description
1	9	ACH7/P0.7/PMOD.3	24	54	AD6/P3.6	47	31	P1.6
2	8	ACH6/P0.6/PMOD.2	25	53	AD7/P3.7	48	30	P1.5
3	7	ACH2/P0.2	26	52	AD8/P4.0	49	29	HSO.1
4	6	ACH0/P0.0	27	51	AD9/P4.1	50	28	HSO.0
5	5	ACH1/P0.1	28	50	AD10/P4.2	51	27	HSO.5/HSI.3
6	4	ACH3/P0.3	29	49	AD11/P4.3	52	26	HSO.4/HSI.2
7	3	NMI	30	48	AD12/P4.4	53	25	HSI.1
8	2	EA	31	47	AD13/P4.5	54	24	HSI.0
9	1	VCC	32	46	AD14/P4.6	55	23	P1.4
10	68	VSS	33	45	AD15/P4.7	56	22	P1.3
11	67	XTAL1	34	44	T2CLK/P2.3	57	21	P1.2
12	66	XTAL2	35	43	READY	58	20	P1.1
13	65	CLKOUT	36	42	T2RST/P2.4	59	19	P1.0
14	64	BUSWIDTH	37	41	$\overline{BHE}$/$\overline{WRH}$	60	18	TXD/P2.0/PVER/SALE
15	63	INST	38	40	$\overline{WR}$/$\overline{WRL}$	61	17	RXD/P2.1/PALE
16	62	ALE/$\overline{ADV}$	39	39	PWM/P2.5/PDO/$\overline{SPROG}$	62	16	$\overline{RESET}$
17	61	$\overline{RD}$	40	38	P2.7	63	15	EXTINT/P2.2/$\overline{PROG}$
18	60	AD0/P3.0	41	37	VPP	64	14	VPD
19	59	AD1/P3.1	42	36	VSS	65	13	VREF
20	58	AD2/P3.2	43	35	HSO.3	66	12	ANGND
21	57	AD3/P3.3	44	34	HSO.2	67	11	ACH4/P0.4/PMOD.0
22	56	AD4/P3.4	45	33	P2.6	68	10	ACH5/P0.5/PMOD.1
23	55	AD5/P3.5	46	32	P1.7			

Figure 2.3. Pin layout and assignment for the A8797BH microcontroller (Intel Corporation, 1986).

2.2.2 Memory

The IS makes use of the whole 64 kbyte memory map which is directly addressable by the 8097 microcontroller. As seen in Figure 2.4, part of this memory map is used by internal 8097 registers and EPROM. The rest of the memory map physically consists of two 43256 RAM chips which are 32 kbytes each. One chip contains all of the odd addresses and the other contains all of the even addresses. Internal 8097 memory overlaps parts of the two 43256 RAM chips, therefore part of the physical memory is wasted. Only the upper 48 kbytes of the RAM chips is used for impact data storage.

The address latches on the digital board are used to latch the RAM memory addresses when they are present on the data/address bus of the microcontroller.

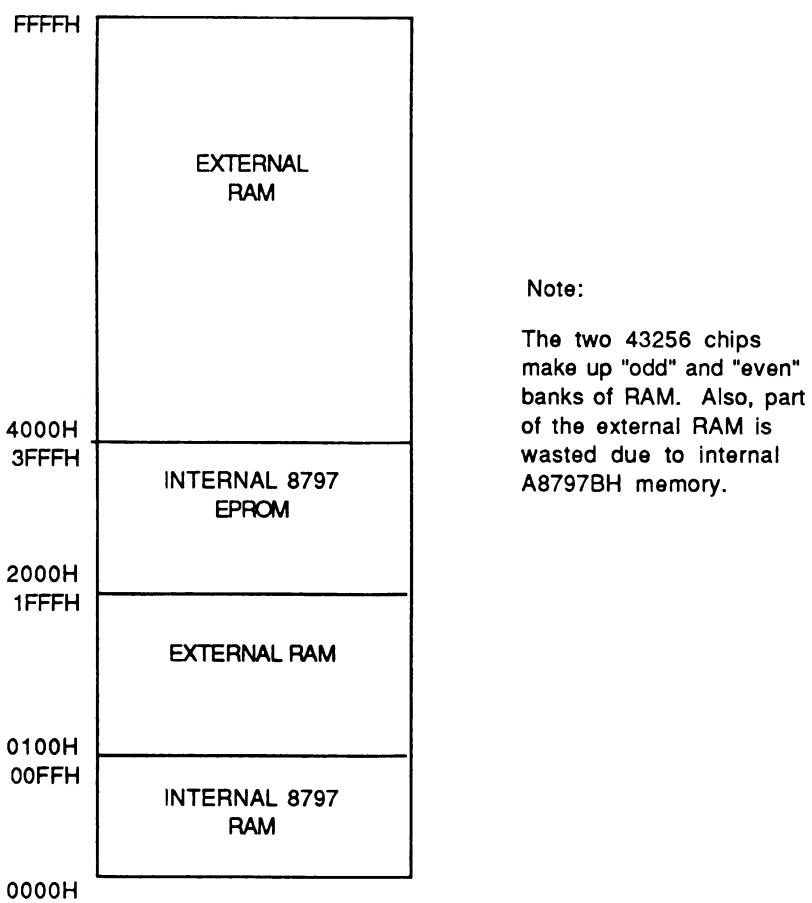

Figure 2.4. Memory organization of the IS.

2.2.3 Power Supply

Power for the IS circuits is provided by two rechargable 6V lead acid batteries (1.2 Amp hour each) connected in parallel. These batteries will last 4.6 hours with the IS drawing approximately 260 mA The IS power supply provides four different voltage potentials: +5V, -5V, -15V, and +2.5V. These potentials are obtained by the use of two voltage regulators, one voltage converter, and a resistor divider (Figure 2.5). The first voltage regulator which is connected to the batteries is also used as an on-off switch with the control pin being accessible via the external 5 pin connector.

2.2.4 Accelerometer and Analog Processing

The analog section consists of a triaxial piezoelectric accelerometer and conditioning circuits (Figure 2.6). The conditioning circuits scale and bias the signal voltages to the range of 0V to 5V for conversion by the A/D aboard the 8097 microcontroller.

The triaxial piezoelectric accelerometer used by the IS contains a Field Effect Transistor (FET) charge amplifier for each axis and therefore requires a constant current source for linear operation. The constant current source is provided by using a diode in the biasing circuit. The output of the accelerometer is AC coupled to an integrated amplifier and 3rd order low pass filter circuit (MF6). The gain of the MF6 is set to one while the cutoff frequency is set to 1000 Hz. The output of the MF6 is AC coupled to the A/D converter on the microcontroller which is biased to +2.5V by a 1 megohm load.

With the accelerometer biasing circuit used in the IS, the accelerometers are capable of measuring acceleration levels between -250g and +250g with a sensitivity of 10 mV per g. The signal coming

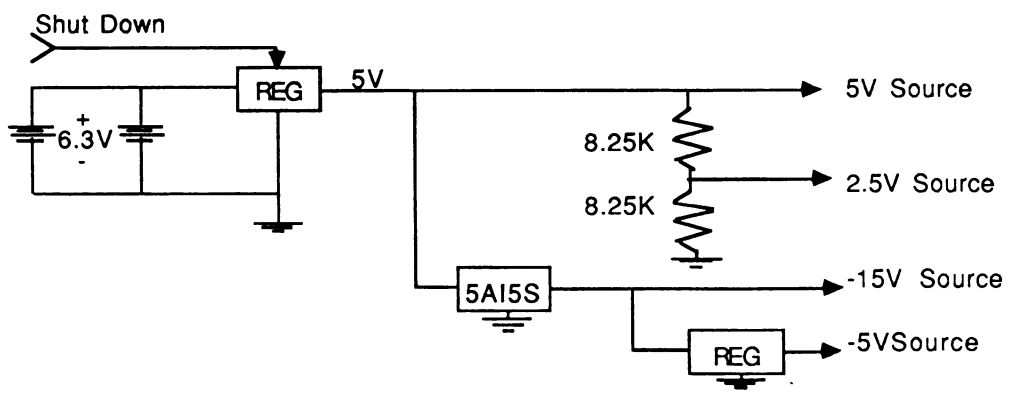

Figure 2.5. Power supply circuit for the IS.

directly out of the MF6 has a range of -2.5V to +2.5V. The biasing voltage of +2.5V which is applied just before the A/D converter, shifts this range so that it is between 0V and +5V. Therefore 0g corresponds to +2.5V at the A/D converter.

The circuit shown in Figure 2.6 is replicated three times; once for each axis. The outputs from the three analog processing circuits are connected to the first three A/D channels of the 8097 microcontroller (AD0 - AD2). All of these input are referenced to a 0V to +5V reference.

2.2.5 Interface Box

In order to charge the IS or communicate with it, an external interface box is used which contains a RS232 driver, a RS232 receiver, an on/off switch, and a 6V battery charger. This interface box is connected to the IS via the five pin connector. The interface box also has a DB25 connector following RS232 standards which can be connected to a terminal or personal computer for serial communications. The interface box is powered from a 120V AC power line.

2.3 Instrumented Sphere Software

2.3.1 Overview of Software

The IS software consists of fourteen modules, seven of which were written in PLM96 (a compiler language) and seven in ASM96 (an assembly language). The software modules contain 41 subroutines for simplicity in maintenance and debugging. Four of the subroutines are interrupt service routines (ISR). The software requires 6.5 kbytes of EPROM.

When the 8097 microcontroller is reset, the monitor program is started by executing the subroutine BOOT which initializes control registers and the serial port. After BOOT has executed, the

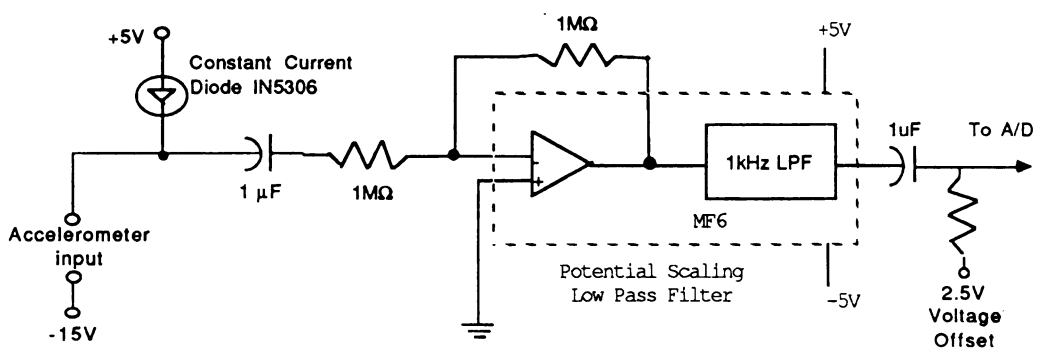

Figure 2.6. Accelerometer and analog signal processing circuit.

main program loop is entered. Interactive commands for the IS are entered from a host computer or terminal through the serial port. IS commands are character strings (keywords) ending with a carriage return. The syntax for the keyword strings and the entry point addresses are stored in a table located in EPROM. Upon reading a possible keyword from the serial port, any leading spaces are removed and the string is compared with the table of keywords until a match is found. Only spaces or a carriage return are allowed to trail the keyword. If no match is found, an error results. If the string of characters matches a keyword, the subroutine corresponding to the keyword is executed, Figure 2.7.

The software contains four keywords: RDATA, SEND, BAUD, and DISPLAY. RDATA is used to initiate or terminate data collection and to change sampling parameters. SEND is used to send a data file to a host computer and BAUD is used to change the serial port baud rate. DISPLAY is used to display memory contents in hexadecimal format for debugging.

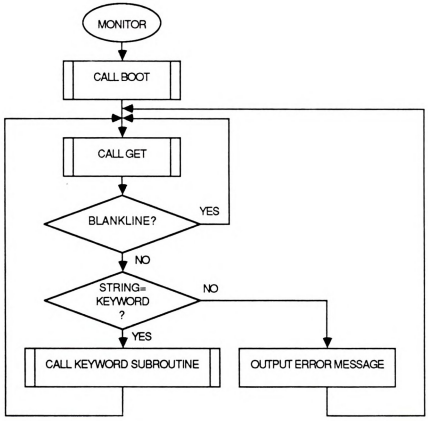

Figure 2.7. Flow chart for monitor program.

The interactive commands of the IS are tree structured. Commands at the top level are keyword oriented, while commands under the top level are menu oriented (a single character executes the command). The top level keywords prevent false commands while connecting or disconnecting the serial line. The subroutines corresponding to the keywords may also be considered separate programs due to their modular design.

2.3.2 Sampling Software

Digitized data are stored in memory in the form of a packed record file (Figure 2.8). This file is made up of a file header and a variable number of records, one record for each impact. The file header contains the time of file creation, the sampling rate, acceleration scale factor and the threshold setting value. Each record consists of a data point count (2 bytes), record start time (4 bytes) and a variable number of acceleration vectors (each 3 bytes long, 1 byte per coordinate direction).

The basic process control for sampling is illustrated in Figure 2.9. The sample timing is handled by the High Speed Output (HSO) Unit which is part of the 8097 microcontroller. The 8097 has an architecture such that the HSO Unit is nearly independent of the main processing unit, Figure 2.10. The HSO Unit has 8 program registers which hold both commands and associated commencement times (Intel Corporation, 1986). All 8 programmed times are continuously compared with a reference timer (timer period = 2.4 μs, using a 10 MHz crystal) and acted upon accordingly. The HSO Unit is programmed by writing to the HSO Unit's registers. For the present application the HSO Unit is programmed to trigger A/D conversions for each coordinate axis and also to trigger a software (HSO) interrupt. HSO Unit instructions are deleted from the HSO registers after execution, requiring that the HSO registers be reprogrammed after each sample period. The sampling process is made self-perpetuating by having the HSO interrupt service routine reprogram the HSO unit after each sample period. A timing diagram of the sampling sequence is shown in Figure 2.11.

After each A/D conversion, an interrupt service routine moves the digital values to a temporary buffer, checks the threshold level and arms the next A/D channel. The triaxial data are saved in RAM if one or more of the channels is above the set threshold. Except during the execution of the HSO interrupt

03	Month	Date	File Header
06	Day		
57	Year		
0A	Hour	Time	
04	Minute		
00	Second		
8A	Sample Rate Count		
00	.		
84	Positive Threshold		
7C	Negative Threshold		
9B	Timer Freq.		
5B	.		
06	.		
E2	g Scale Factor (must		
4F	be mult. by 1e-4)		
00	.		
04	# Pt. / Impact		1st. Impact Record
00	.		
0E	Start Time Count		
33	.		
05	.		
00	.		
83	X Value	Sample #1	
80	Y Value		
84	Z Value		
83	X Value	Sample #2	
80	Y Value		
84	Z Value		
80	X Value	Sample #3	
82	Y Value		
84	Z Value		
7E	X Value	Sample #4	
81	Y Value		
84	Z Value		
09	# Pt. / Impact		2nd. Impact Record
00	.		
E1	Start Time Count		
39	.		
05	.		
00	.		
80	X Value	Sample #1	
82	Y Value		
84	Z Value		
	Etc...		

Start Time = (Start Time Count * 256) / Time Freq.
[Sec.]

Sample Rate = Time Freq. / Sample Rate Count
[Hz.]

Figure 2.8. Format of the IS data file.

service routine and the A/D interrupt service routine, the main processor is free to handle serial communication or any other processing task.

The HSO Unit was selected to control sample timing rather than a simple program loop, since threshold checking and serial communications would result in unpredictable loop timing. Simple program loop sample timing could also be adversely affected by a new version of the 8097 microcontroller. Using the HSO unit and interrupts does, however, make the sampling routines more complex.

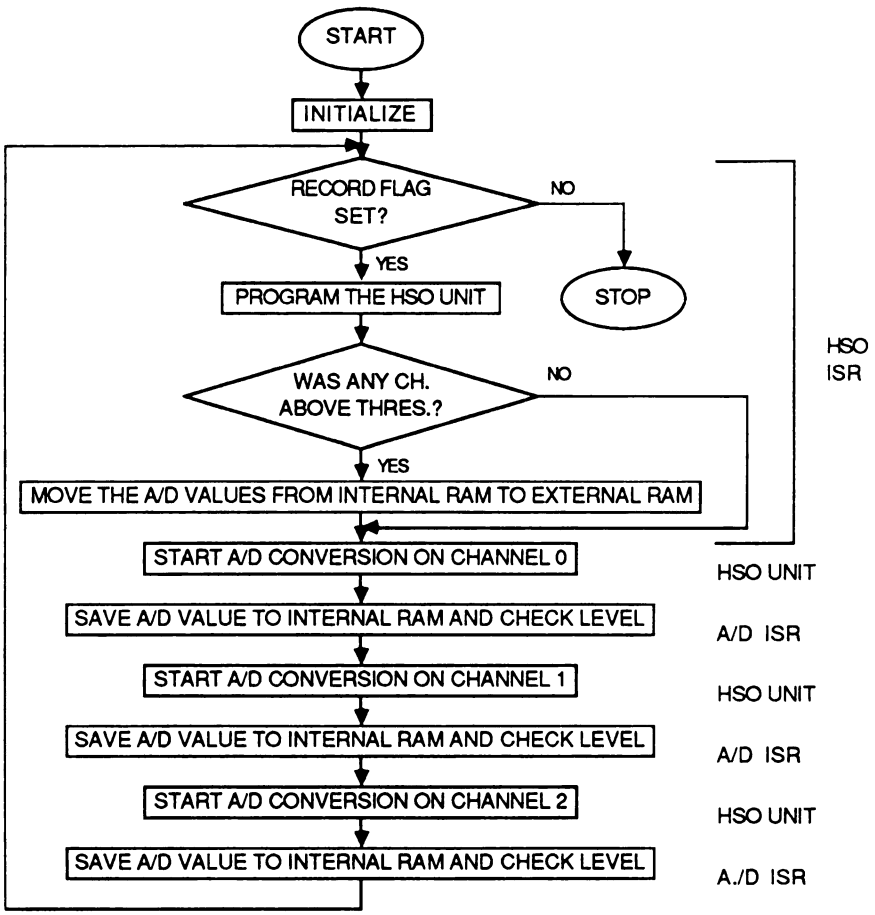

Notes:
1. The RECORD Flag is changed external to this flow chart with RDATA.
2. ISR = Interrupt Service Routine.

Figure 2.9. A flow chart showing the sampling process. The sampling process is implemented by two interrupt service routines and the HSO unit.

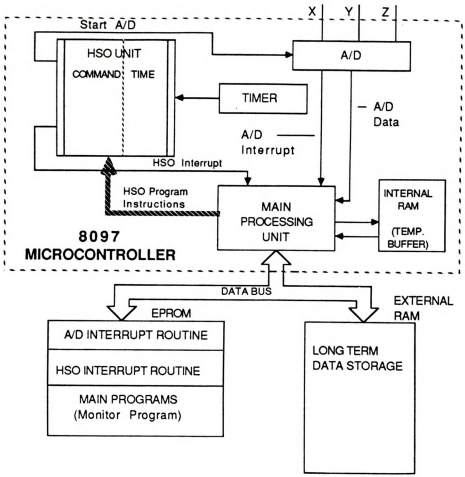

Figure 2.10. Block diagram of the 8097 microcontroller and Instrumented Sphere hardware as related to the sampling software.

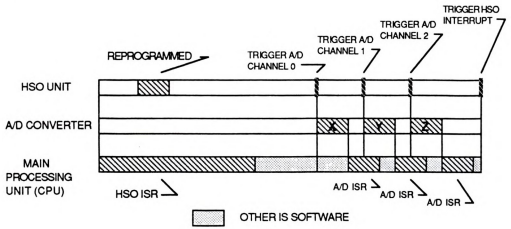

Figure 2.11. Timing diagram for one sampling period.

RDATA is the user interface program for the data collection software. RDATA is a menu driven program which allows the user to start and stop data collection, display the current sample parameters, and change the sampling rate and threshold level. New sampling rates and threshold levels are entered in units of hertz and g's respectively. Due to the limited resolution of the parameter variables, the entered values may be changed slightly by RDATA. Upon starting data collection, RDATA will request the current time and date, so that it can be inserted at the beginning of the data file. Starting data collection also causes the old impact data to be overwritten.

2.3.3 Communication Software

The IS uses the serial port on the 8097 in an interrupt driven mode. A serial port interrupt service routine handles the transfer of bytes between the 8097 serial port (transmit and receive) registers and two, software defined, FIFO buffers (Figure 2.12). The two FIFO buffers are physically located in the internal RAM of the 8097 with the input buffer using 32 bytes and the output buffer using 8 bytes. The serial port interrupt service routine also handles software handshaking (XON and XOFF). The subroutines PUT, GET, BYTEGET, POLL, ECHOON and ECHOOFF are used by the rest of the IS software to add or remove data from the FIFO buffers. The data flow for the serial communications is shown in Figure 2.13.

Block oriented I/O is supported through the PUT and GET subroutines. Memory for two 42 character strings (IN and OUT) is reserved in external RAM for the purpose of assembling and scanning I/O blocks. GET, when called, reads characters from the FIFO input buffer and writes them sequentially to IN until a carriage return is encountered (Figure 2.14). GET allows the input block to be edited by interpreting the ASCII backspace or delete characters to mean that the previous character should be deleted. If the echo flag is on, GET echoes the characters as they are read to the FIFO output buffer; this produces the effect that the user sees on the screen what is being typed from the keyboard. PUT simply copies a specified number of characters from the output block to the FIFO output buffer (Figure 2.15). The subroutines ECHOON and ECHOOFF turn the echo flag on or off.

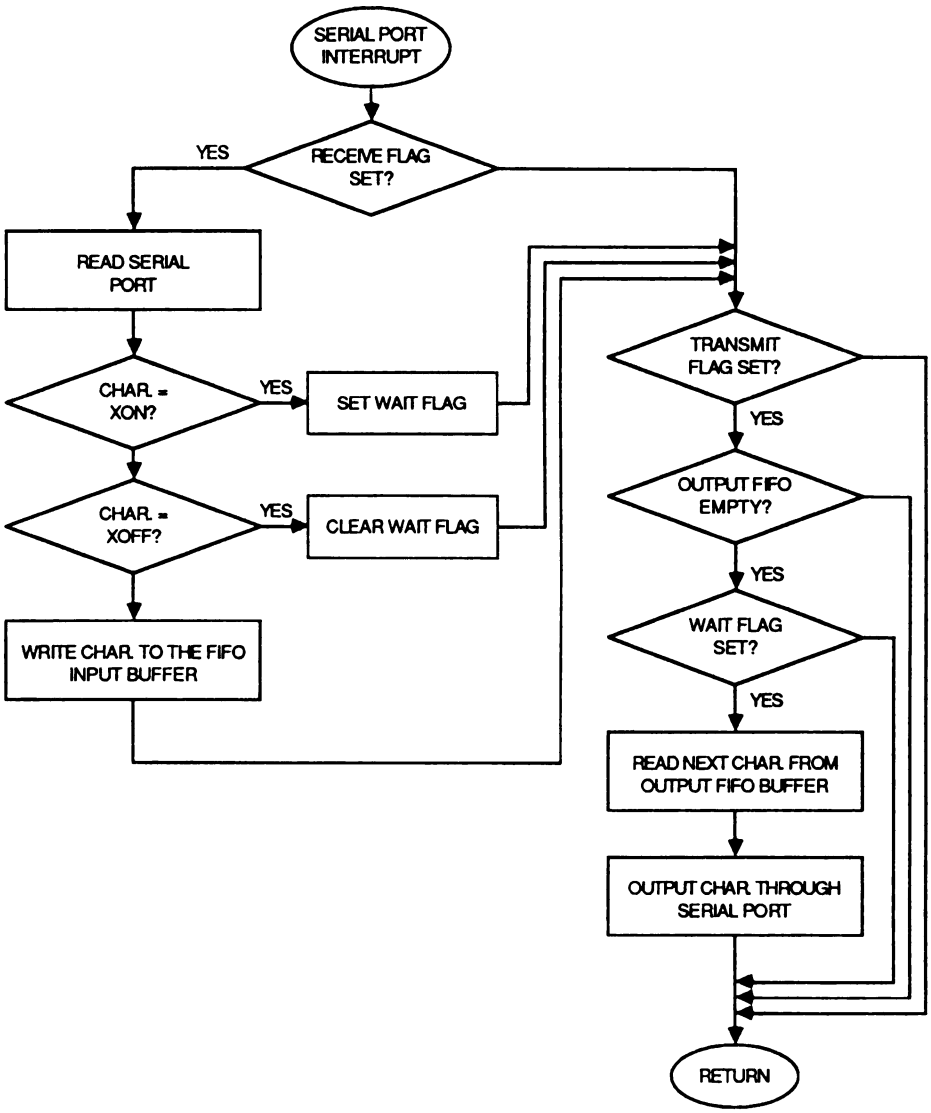

Figure 2.12. Flow chart of the serial port interrupt service routine.

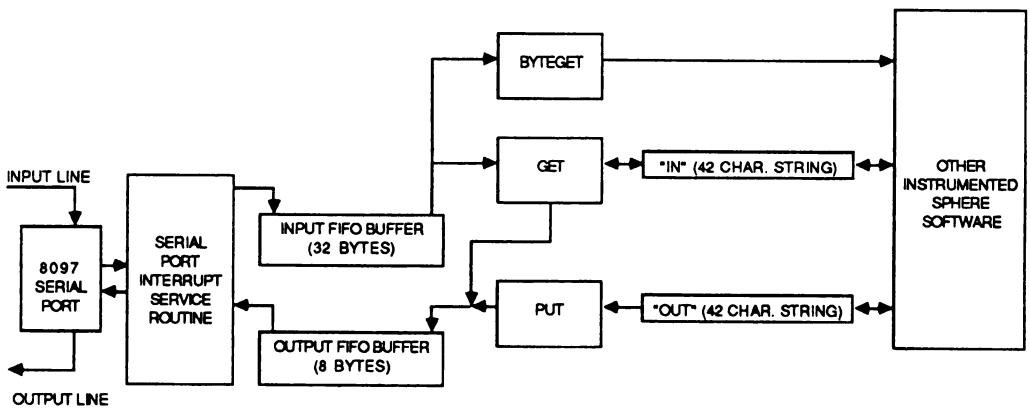

Figure 2.13. Data flow diagram for IS serial communications.

The subroutines BYTEGET and POLL are used for byte oriented I/O without echo. BYTEGET simply reads bytes one at a time from the FIFO input buffer and POLL is a boolean function that is used to check the status of the FIFO input buffer.

The default baud rate for the IS is 1200 baud, however the baud rate can be changed by executing the routine BAUD. BAUD will display a menu which allows the baud rate to be changed to one of the following rates: 300, 1200, 2400, 4800, and 9600 baud.

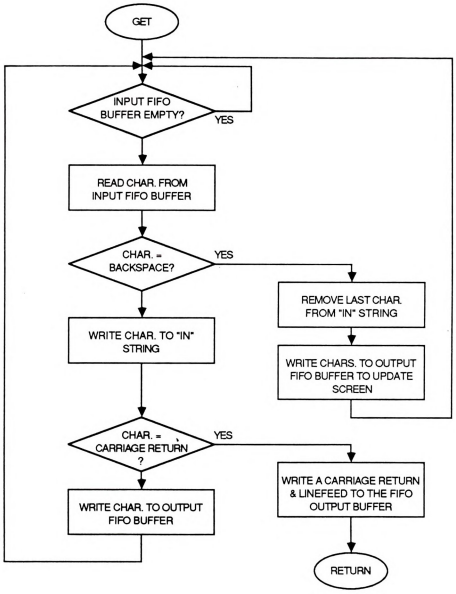

Figure 2.14. Flow chart of the GET routine.

In order to transmit the impact data to a host computer, the SEND routine must be executed. During serial data transfer the 8-bit data bytes are converted to two hex digits, so the ASCII character for each hex digit can be used in data transfer. The ASCII carriage return and line feed characters follow the two hex digits expressed in ASCII. Using the above data conversion, transferring one 8-bit data byte requires four ASCII characters. Converting the data to ASCII is necessary in the use of software handshaking. Assuming that the host computer does not interrupt data transmission via XON/XOFF handshaking, 27 min. would be required to transfer the IS's 48 kbyte data buffer using a 1200 baud transmission rate.

SEND, upon starting execution, will send a message showing the number of bytes in the data buffer and will prompt for a carriage return to start data transmission or a control-C to abort SEND. During this prompt the user should open a capture file on the host computer.

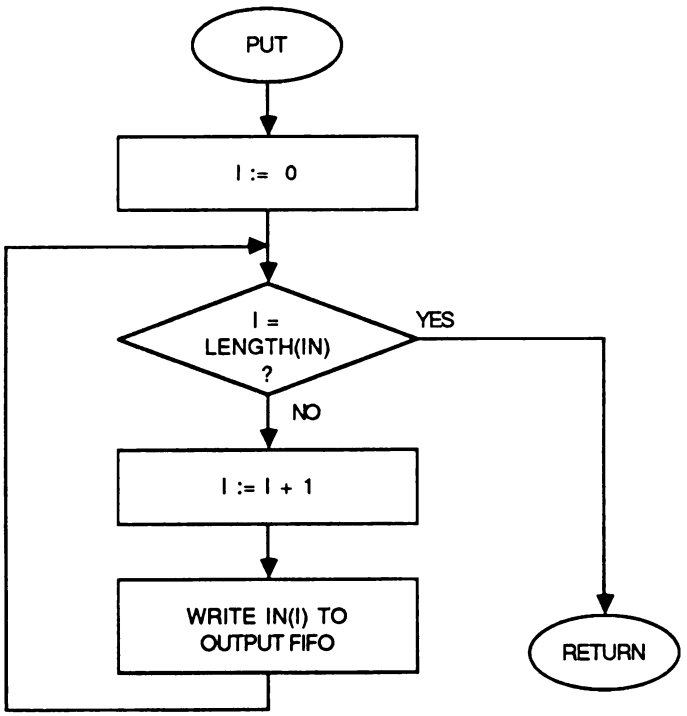

Figure 2.15. Flow chart of the PUT routine.

2.3.4 Other Utility Routines

The IS software also contains routines for keeping track of real time, number format conversions, and data memory management. The CLOCK interrupt service routine, which increments software counters when the 16-bit hardware timer overflows (every 0.157286 s with the 10 MHz crystal), keeps track of real time. Four bytes are alloted for the software counters which allows the IS to keep track of time for 7818 days before the counters wrap around. However the data collection routine uses only three of the bytes; allowing only 733 hours (30 days and 13 hours) before wrap around. The fourth time byte used by the data collection software is the high order byte of the hardware timer.

The IS system software contains several subroutines to convert internal binary numbers to ASCII format or vice versa. The IEEE floating point format is also included in the conversion routines even through the IS software does not use floating point numbers due to the large amount of memory required for the math library. The binary number involved in the conversion process is stored in a non-relocatable five byte block of memory while the ASCII formatted number can be a string located anywhere in memory.

The subroutine FORMIN handles all ASCII to binary conversions and informs the calling program about the type of conversion made through a status byte. The status byte is also used to flag format errors. The binary number resulting from FORMIN may be one of the following types: byte, word, short integer, integer, double word, and real. FORMIN assumes that the base-10 number system has been used and that the ASCII string may be in scientific notation or fixed point notation.

The subroutine FORMOT is used to convert an internal binary number to an ASCII string. If the binary type is byte, word, short integer, or integer; the resulting ASCII string is in fixed point form; otherwise scientific notation is used. When calling this subroutine, the original binary type must be specified along with the address for the resulting string.

WHEX, a third subroutine, is used to convert a variable of type "byte" to a hexadecimal notation ASCII string. This subroutine is used by SEND and DISPLAY. When calling this routine, the output string address must be specified as a parameter.

The subroutine DISPLAY is used to display memory contents starting at address 4000H by the page (256 bytes at a time) in hexadecimal notation. After a page of memory has been displayed, the next page may be displayed by entering the character "D", or DISPLAY may be exited by entering the character "E". The output from DISPLAY is formatted to fit on a 40 character wide terminal screen.

Near the beginning of software development, it was envisioned that the IS might have more than one data buffer; therefore subroutines were developed to open and close data buffers (files). Several variables have been assigned for memory management and include: two file pointers, a file length counter, a start of file address variable, and a file length limit variable.

The subroutine WRITE, which is similar to Basic's "Print" statement was written to aid in writing messages to the terminal screen. WRITE differs from the "Print" statement in that it can only output ASCII text. The address of an ASCIIZ string (an ASCII string with the last character being the null character, 00H) must be specified when calling WRITE. However PLM96 allows the defining of a constant string while specifying it's address as a parameter to a subroutine, which resulted in an easy to use programming tool.

2.3.5 Sampling Rate Analysis

To determine the maximum sampling rate of the IS, the software execution times and A/D conversion time must be found. Software execution times are determined by totaling the microcontroller state times required to execute the program instructions. A state time for the 8097 equals 3 crystal cycles. Table 2.1 shows the state times required by subroutines running during data collection.

The A/D conversion time of the EPROM version of the 8097 microcontroller is 26.4 μs. As shown in Figure 2.11, A/D conversions occur three times during each sample period; once for each axis. The real time clock routine may or may not be executed during a given sample period, but time must be allocated for situations when it is. Allowing no overlap between sampling tasks, the minimum sample period in microseconds, is calculated in Equation [2.1]. By inverting the result of Equation [2.1], the sampling frequency is shown in Equation [2.2].

$$121 + 31 + 3(35) + 3(26.4) = 336.2\mu s \qquad [2.1]$$

Table 2.1. The execution times for subroutines running during data collection (using 10 a MHz crystal).

SUBROUTINE	STATE TIMES	TIME (μs)
HSO interrupt service routine	404	121
REAL TIME CLOCK	103	31
A/D interrupt service routine	117	35
(A/D value saved)	(56)	(17)

$$1 / 336.2\mu s = 2974 \text{ Hz} \quad [2.2]$$

By overlapping software tasks with A/D conversion tasks, the minimum sample period is reduced and the frequency is increased as shown in Equations [2.3] and [2.4] respectively. However the software used to internally set the sampling rate, reduced the maximum rate to 3466 Hz to allow for unforeseen circumstances.

$$121 + 31 + 3(17) + 3(26.4) = 282.2\mu s \quad [2.3]$$

$$1 / 282.2\mu s = 3544 \text{ Hz} \quad [2.4]$$

Adding the A/D conversion and the A/D interrupt service times together, a minimum of 43.3μs is required between sampling each axis. Additional sampling speed can be achieved if one can accept a few incorrect sample values occurring at the beginning and end of an impact. This is possible, since the HSO interrupt service routine has less instruction code to be executed during the middle of impacts.

2.4 Instrumented Sphere Case

The IS case is made up of three pieces: two partially hollow hemispheres and a flat plate which is fitted between the hemispheres (Figure 2.16 shows an exploded view of the case and electronic hardware). All three pieces of the case were machined from epoxy (Ad-Tech Plastic Systems Corp. EC-420) castings. The EC-420 has the following physical properties: Hardness Shore D = D-70; Tensile Strength = 41.4 MPa (6000 psi); Elongation = 10%; and is water white clear. After installing the electronic hardware, all voids in the case were filled with bees wax. The three pieces of the case were fastened together with four self tapping screws.

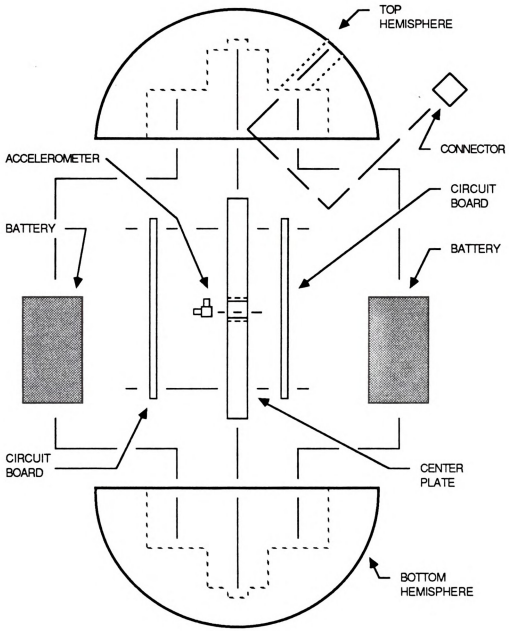

Figure 2.16. Exploded view of the IS case.

As seen from the side view in Figure 2.17, the flat plate piece of the IS case is rotated 45 degrees and fitted into a friction fit slot when the case is assembled. The accelerometer and both circuit boards are mounted to this flat plate with screws and nuts. A hole was cut in the center of the plate for the accelerometer which was mounted with a stud as shown in Figure 2.17. Holes were drilled through the flat plate in order to electrically connect the two circuit boards.

As seen in Figure 2.16, pockets were cut into both hemispheres for the batteries, with one battery being held on each side of the flat plate. The five pin connector was fastened to the IS case by milling a hole into one of the hemispheres and mounting it from inside with screws. Wires were then run to the circuit boards.

Bees wax was added to the IS case after it was assembled through a hole in one of the hemispheres. The purpose of the bees wax was to prevent internal vibration and provide solid mechanical interfaces. The wax which melts at 60° C was poured into the IS.

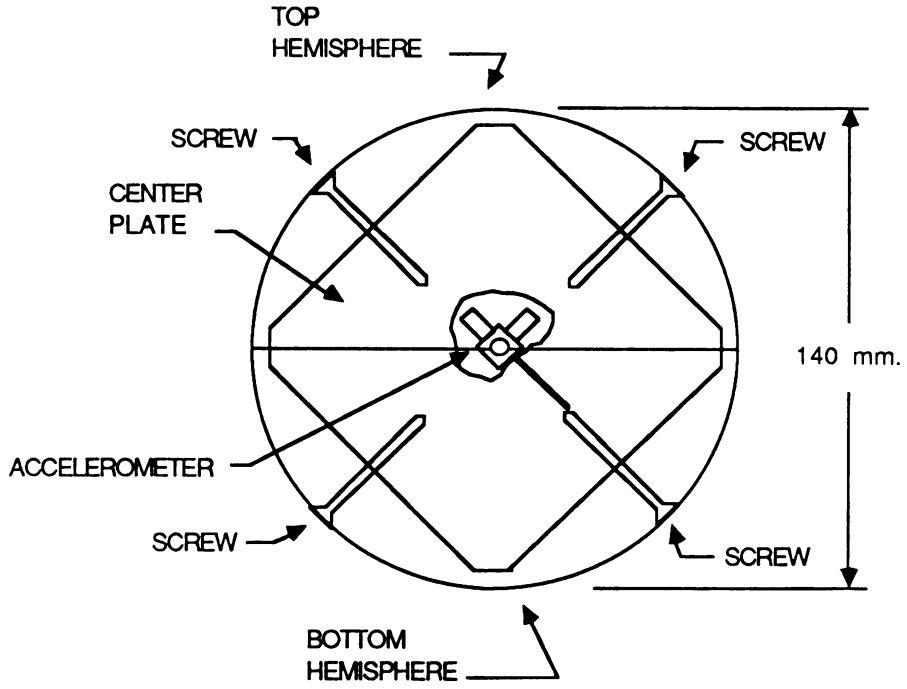

Figure 2.17. Side view of the IS case.

2.5 Instrumented Sphere Performance

2.5.1 Sampling Rate Verification

The sampling rate accuracy, as related to the data collection algorithms, was test by sampling a known sine wave signal. These tests were run on an older version of the IS hardware as originally described by Siyami et al. (1986). The only significant difference between that system and the present is the crystal; the old version had a 12 MHz crystal while the present version has a 10 MHz crystal. Therefore the sampling rate results should be reduced proportionally.

The sampling software was tested at five different sampling rates (using the 12 MHz crystal): 3012Hz, 3521Hz, 3817Hz, 4167Hz and 5000Hz. These sampling rates were used because they are near or above the maximum sampling rate.

The period of a 10 Hz sine wave (0.1 s) was used as the reference time and was applied to the IS by replacing the accelerometers with a signal generator. For collecting the sine wave data, the thresholds were set to zero so that the whole sine wave could be recorded. Memory overflow was prevented by collecting for only 3 s. The results of the tests showed that the number of samples recorded in the 0.1s periods varied by ±1 bit, from the ideal number of samples. This can be explained by the quantization error and thus the sampling rate accuracy was verified.

2.5.2 Scale Calibration

Scale calibration was performed dynamically by placing the IS on an impact table along with a calibrated accelerometer connected to a digitizing oscilloscope (Figure 2.18). Since the IS and the calibrated accelerometer were both attached to the table, each experienced the same acceleration upon impact and therefore the peak values could be used for calibration. Half sine impacts with durations of 5-6 ms were used for the calibration tests. The calibrations of the three axes were handled separately by placing the the IS on the impact table such that only the desired axis received the main impact. Ten drops were made with each of the six possible orientations from five different drop heights. During analysis of the calibration data, the co-linear (positive and negative orientations) data were combined to produce only one set of calibration factors for each axis. During the calibration tests the sampling rate (3333 Hz) of the digitizing oscilloscope and the IS were matched but not synchronized. By matching the

sampling rates, the instantaneous probability of missing the true peak is equally likely for the IS and the oscilloscope. Averaging over twenty tests will assure unbiased calibration values.

The data measured by the IS was processed using the program TESTSYS (described in section 3.2) in order to find the peak values. The peak values from the calibrated accelerometer were found by using the "peak function" which is built into the digitizing oscilloscope. The peak values from the IS and from the calibrated accelerometer were entered into a commercial statistical package for linear regression analysis. The coefficients B(0) and B(1) in Equation [2.5] from the linear regression analysis are listed in Table 2.2. The linear regression curves are shown in Figures 2.19. to 2.21

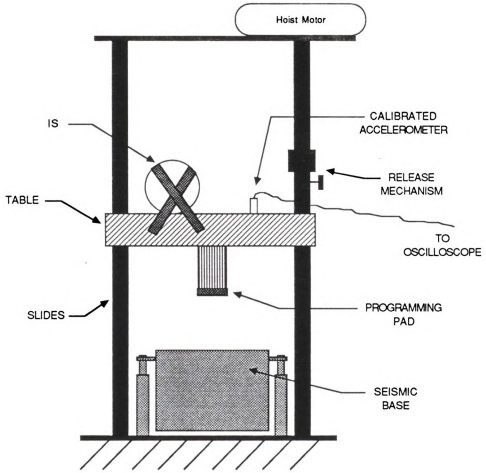

Figure 2.18. The impact table used in the calibration procedure.

Table 2.2. Linear regression results from IS calibration.

Coefficient Name	Regression Coefficient	Standard Error	Confidence Limits(3s) Lower	Upper
X-Axis				
B(0)	-0.99	1.30	-4.90	2.90
B(1)	2.17	0.0224	2.10	2.24
Y-Axis				
B(0)	2.04	1.50	-2.46	6.54
B(1)	1.99	0.0240	1.92	2.06
Z-Axis				
B(0)	3.81	1.42	-0.45	8.07
B(1)	2.08	0.0232	2.01	2.15

Correlation between data and regression line = 0.999 for all three axes.

$$Y = B(0) + B(1) * X \qquad [2.5]$$

where:

Y = acceleration in units of g

B(0) = Bias (Y intercept)

B(1) = scale factor from digital counts to g

X = Digital counts from IS

The error percentages for each axis when measuring a 50 g impact were calculated by solving Equations 2.6 to 2.10, and the results are listed in Table 2.3.

$$50 = B(0)_{Regr} + B(1)_{Regr} * X_{Regr} \qquad [2.6]$$

$$50 = B(0)_{Up} + B(1)_{Up} * X_{Low} \qquad [2.7]$$

$$50 = B(0)_{Low} + B(1)_{Low} * X_{Up} \qquad [2.8]$$

$$\%\ error_{Low} = (X_{Low} - X_{Regr}) / X_{Regr} \qquad [2.9]$$

$$\%\ error_{Up} = (X_{Up} - X_{Regr}) / X_{Regr} \qquad [2.10]$$

Not all of the error shown in Table 2.3 is due to inaccuracies in the IS, but is partially due to the calibration technique since the errors in Table 2.3 were calculate based on the standard errors from the

Table 2.3. Error summary for the IS.

Axis	% $error_{Low}$	% $error_{Up}$	% $error_{Avg}$
X	-11	+11	±11
Y	-9	+13	±11
Z	-12	+13	±12.5

linear regression analysis. Part of the standard errors from the analysis were due to missing the peaks with the IS and oscilloscope.

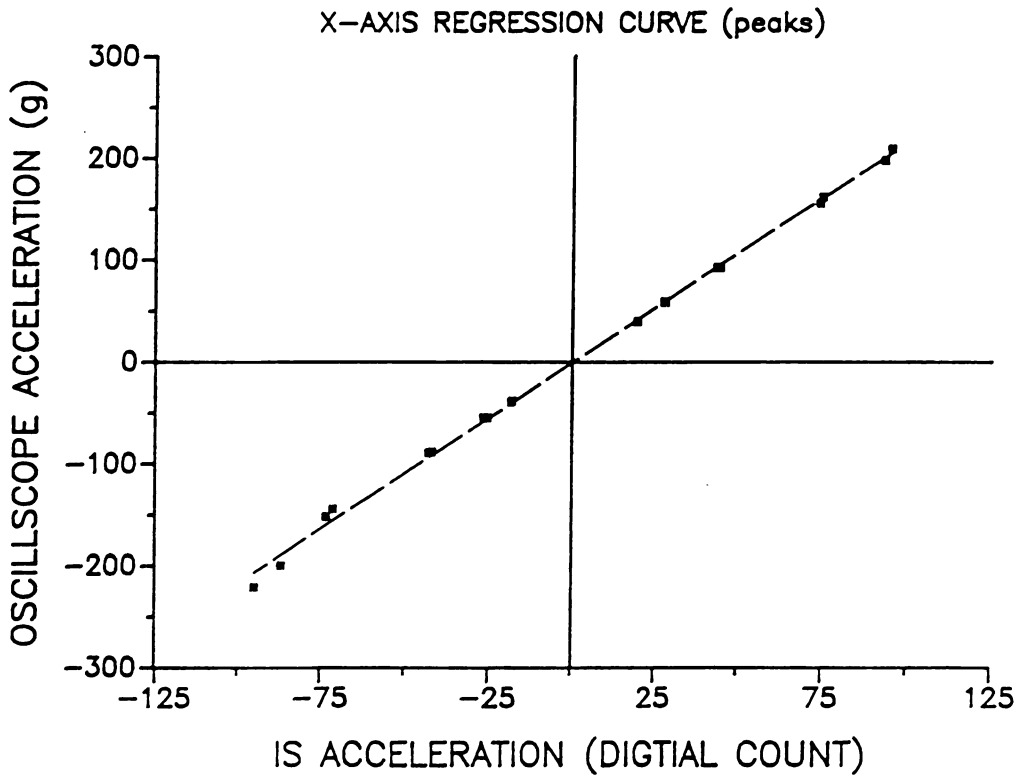

Figure 2.19. Linear regression curve for the X-axis of the IS.

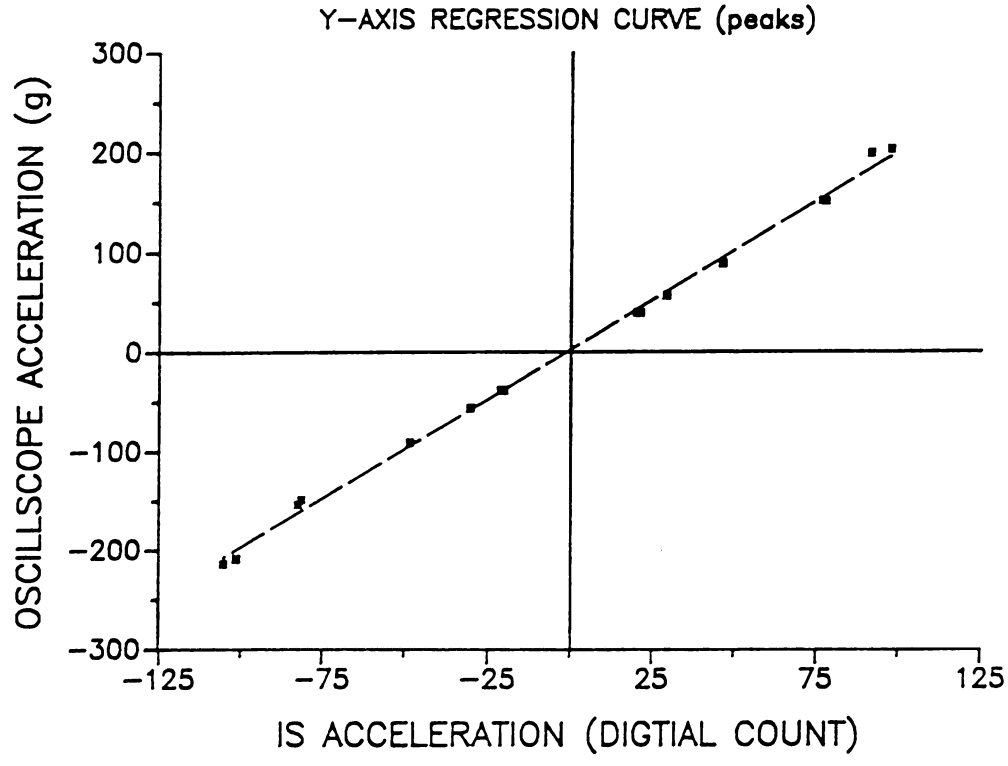

Figure 2.20. Linear Regression curve for the Y-axis of the IS.

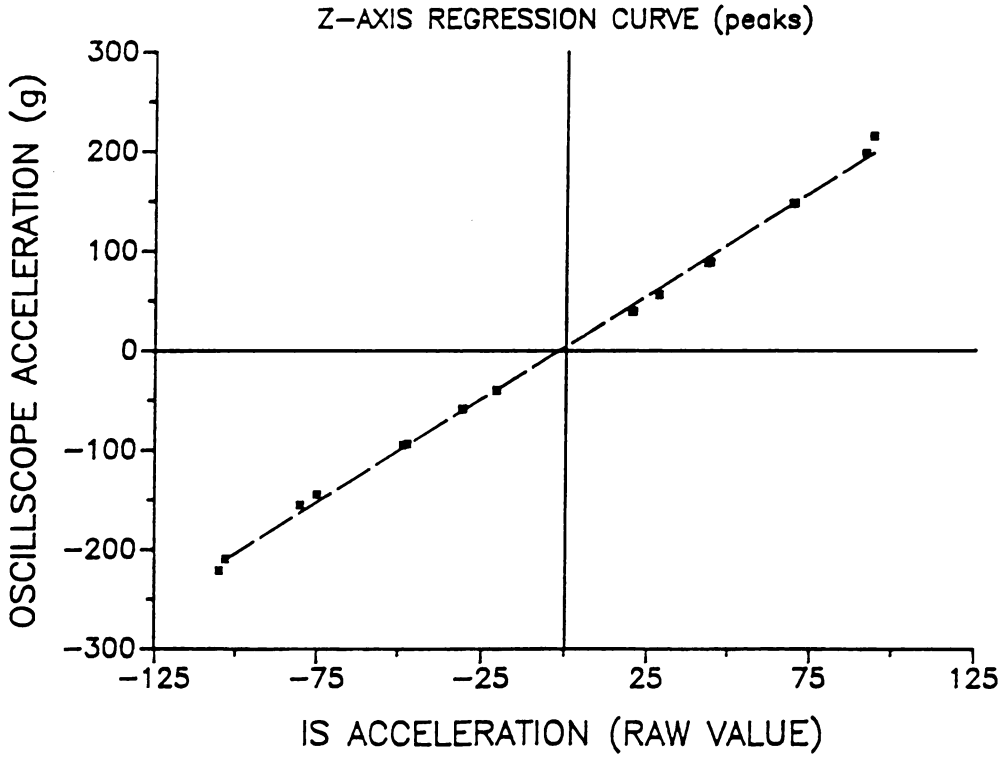

Figure 2.21. Linear Regression curve for the Z-axis of the IS.

3. Impact Data Analysis

3.1 Previous Work on Impact Modeling

Many of the researchers working with impact modeling have designed, built, and instrumented their own drop-testers. Hammerle and Mohsenin (1966) built a moving-mass, fixed-specimen drop-tester. For instrumentation they mounted an accelerometer to the moving mass and attempted to use a double integrating analog computer to analyze the acceleration signal, they had trouble however calibrating the analog computer and it was used only to show relative relationships. They had hoped that the analog computer could generate the velocity and displacement traces from acceleration data. Hammerle and Mohsenin also used their drop tester to find the coefficients of restitution for various padding materials by inserting drop heights (H_R) and rebound heights (H_D) into the following equation:

$$\text{Coefficient of restitution} = \text{sqrt}(H_R / H_D) \qquad [3.1]$$

For Latex foam (28.6 mm to 50.8 mm thick), the most extensively tested material, it was found that the coefficient of restitution decreased as drop height increased and was between 0.86 and 0.37 for 0.218 m to 1.356 m drops. Hammerle and Mohsenin also worked with energy balance relationships and developed a technique for finding the energy absorbed by fruit during impact. The method involves dropping both a rigid metal sphere and a fruit onto the same surface. By assuming that the metal sphere absorbs no energy during the impact with a much softer material, rebound energies can be used to determine the energy absorb by the fruit as shown in Equation [3.2].

$$E_{absorbed} = E_{rebound\ sphere} - E_{rebound\ fruit} \qquad [3.2]$$

Fluck and Ahmed (1973) also did a series of tests using a falling-mass drop-tester with an accelerometer attached to the falling mass. Displacement was also recorded by using high speed photography. The acceleration wave forms which were displayed on the ocilloscope were also recorded

by a camera. From tests, Fluck and Ahmed found that the peak acceleration did not always occur at the same time as peak displacement. One of their experiments consisted of dropping a 732 gram mass from 80 mm onto green peppers, oranges, limes, tomatoes, lemons, squash, cucumbers and peaches. The average impulse for the drops was 1.1 kg m per s with the peak acceleration varying from 11 g to 33 g and with durations ranging from 26 ms to 9 ms respectively. Fluck and Ahmed also observed that acceleration curves for damaged fruit were more jagged then those for undamaged fruits. It was proposed that tissue failure caused the sudden changes in acceleration and force.

Chen et al. (1985) developed an impact instrumentation interface for a personal computer to record accelerometer data. Chen used a 43.2 gram steel rod with a 19 mm diameter spherical tip for impacting the fruit. This steel rod also contained an accelerometer to sense the acceleration during impact. The other information used by Chen's analysis routines was entered by the user and included: mass of the impacting rod and drop height. Drop height was necessary to calculate the impact velocity from the free fall equation. By using the impact velocity as an integration constant, the acceleration data were integrated to attain velocity and displacement as functions of time. Force was found by multiplying the acceleration by the mass of the steel rod. Force multiplied by displacement was also integrated to find energy relationships. Chen was also able to make plots of force vs. deformation which showed the expected hysteresis.

$$m\dddot{x} + (mk/c)\ddot{x} + k\dot{x} = 0 \qquad [3.3]$$

Damage reduction has not been the only reason for studying impacts to agricultural products. Nahir et al. (1986) studied the impact responses of tomatoes for the purpose of grading them for ripeness by using stiffness as a gauge. The tomatoes were dropped from a low height onto a force transducer which measured the impact. The Maxwell solid model (Equation [3.3]) was used in order to relate the stiffness or spring constant to the impact force data. After solving the differential equation, the spring constant (k) can be found by the following equation:

$$k = \frac{I \pi^2}{T^2 V_o H^2 (1 + e_r)} \qquad [3.4]$$

where:

I = impulse

T = impact duration

V_o = impact velocity

H = constant dependent on the number of degrees of freedom and on the fruit damping effect

e_R = coefficient of restitution

Nahir's results showed the calculated k to be within 5% of the actual stiffness.

Some of the impact modeling was done from the material deformation point of view. Horsfield et al. (1972) expanded on Timoshendo and Goodier's (1951) extended Hertz's contact theory for two impacting spheres by applying it to the study of peach damage. In order to use the extended Hertz theory, they assumed the following:

1. The material of the contacting bodies is homogeneous.
2. The loads applied are static.
3. Hooke's law applies.
4. Contacting stresses vanish at the opposite ends of the body (semi-infinite body).
5. The radius of curvature of the contacting solid is very large compared with the radius of the area of contact.
6. The surfaces of the contacting bodies are sufficiently smooth that tangential forces are eliminated.

Using units of inches and lbs. Horsfield's resulting equation is the following:

$$S_y = 0.243 (W h)^{1/5} \left(\frac{E_1 E_2}{E_1 + E_2} \right)^{4/5} \left(\frac{R_1 + R_2}{R_1 R_2} \right)^{3/5} \qquad [3.5]$$

where:

S_y = max. allowable shear stress

W = weight of fruit

h = drop height

E_1 = modulus of elasticity of fruit

E_2 = modulus of elasticity of impact surface

R_1 = radius of fruit

R_2 = radius of impact surface

Horsfield used drop tests to determine E_1 and S_y; E_1 was determined by using low drop heights which did not cause damage while higher drop heights were used to find S_y. Tests were also performed to relate the S_y determined from drop tests to the S_y determined from pressure tests used by horticulturists. From the above equation, it can be seen that maximum shear stress is proportional to an energy term, a modulus term, and a radius term.

Yang (1966) developed a contact force model for viscoelastic bodies from the elastic model developed by Timoshenko and Goodier (1951) by replacing the multiplication of time functions with convolution in the time domain. Yang's analysis used an ellipsoid as the general body shape and was limited to homogeneous, isotropic, linearly viscoelastic materials. Example solutions were given for the problem of a rigid sphere indenting a three-parameter viscoelastic half-space by its own weight and the problem of two contacting incompressible viscoelastic Maxwell spheres.

Hamann (1970) applied Yang's work to apples and gave a detailed solution for the impact of two apples. The Maxwell relaxation modulus used in Hamann's analysis is given by Equation [3.6] while the dynamics equation is given by Equation [3.7].

$$G(t) = G_o\, e^{-(t/tau)} \qquad [3.6]$$

where:

G_o = elastic modulus

tau = relaxation time

$$\ddot{\alpha}(t) + \frac{\alpha(t)}{\tau_1} + C_1[\,\alpha(t)\,]^{3/2} = \frac{V}{\tau_1} + \frac{g}{\tau_1}\,[\tau_1 + t] \qquad [3.7]$$

where:

$$C_1 = \frac{[2\,R]^{1/2}\;G_o}{3M_1\,[1 - \nu^2]}$$

$\alpha(t)$ = approach of bodies

R = radius of curvature of both bodies

τ_1 = relaxation time

G_o = elastic modulus

M_1 = mass of the falling apple

ν = Poisson's ratio

g = acceleration due to gravity

V = impact velocity

Equation [3.7] is valid only from the point of contact to the point of maximum displacement. Since Equation [3.7] is non-linear, a closed form solution was not possible and thus numerical methods were used. Hamann found solutions for both 50.8 mm (2 in) and 314.8 mm (12 in) drops and used the displacement results to calculate internal stresses. For a 50.8 mm drop, surface pressures reached 1407 kPa (204 psi) which was 2/3 of the maximum pressure for a 304.8 mm drop, however the high pressure area was much larger for the 304.8 mm drop. Hamann also found that increased drop heights decreased impact duration and increased maximum displacement.

Franke and Rohrbach (1981) altered the Kelvin-Voigt model, making it non-linear, and applied it to the impact of a sphere on a flat plate (Equation [3.8]).

$$m\ddot{x} + c\frac{v_o}{v_t}\,(1 - e^{-t/\tau})\,\dot{x} + k(x + \gamma(1 - e^{x/\gamma})) = -mg \qquad [3.8]$$

where:

x = displacement

m = mass

k = limiting spring constant

g = constant

τ = constant

g = acceleration due to gravity

The spring constant and damping constant are no longer constants but are "turned on" as the impact proceeds. The justification for the variable spring constant was that the the force-strain curve has a slope of zero at zero displacement but increases to some constant value during the impact. A motivation for the variable damping constant was that the initial slope of the impact force-time curve is non-zero. Another motivation was that for very low impact velocities the coefficient of restitution is nearly one, but decreases as impact velocity increases. Franke and Rohrbach then proceeded to develop an iterative least-squares fit numerical method for finding the non-linear model parameters from measured force data. By using 8-bit resolution force data, their calculated parameters were accurate to two significant figures.

Peleg (1984) used the work of several previous researchers to develop a Boltzmanlike non-linear viscoelastic model for produce damage. Peleg used the work of Timoshenko and Goodier (1951) for the geometric aspects of his model while using Yung's work for the viscoelastic aspects. Peleg's main contribution was to add a pair of non-linear springs and a Coulomb (dry) friction damper. The two springs were in series with each other, while the viscous and Coulomb dampers were in parallel with one of the springs (spring #1). This configuration required a minimum force threshold in order to have motion of the spring-damper portion of the system due to the Coulomb fiction. Another feature of this model was that spring #1 became softer as it was compressed and spring #2 became harder. The system equation is as follows:

$$F = k_1 x_1 + r\, x_1^3 + c\dot{x}_1 + F_f(\operatorname{sgn} \dot{x}_1) = k_2 x_2 + r\, x_2^3 \qquad [3.9]$$

where:

x_1 = displacement of 1st. spring

x_2 = displacement of 2nd. spring

$x_1 + x_2$ = total displacement

F = Force acting on speciment

$kx + r x^3$ = cubic elastic force

$c\dot{x}$ = viscous damping force

$F_f (\text{sgn } \dot{x})$ = internal friction force

r = hardening or softening constant

k_1 = elastic parameter

k_2 = elastic parameter

De Baerdemaeker, Lemaitre and Meire (1982), and Delwiche and Bowers (1985) worked on using the frequency characteristics of the impact force data in order to sort fruit for firmness. Preliminary work was done with 256 point FFT's while later work involved the use of analog bandpass filters. They found that the frequency value which is 20 dB down from the DC level, correlated (0.752) with the elastic modulus and Magness-Taylor value of apples. They also found that the 250 Hz frequency component correlated (0.681) with the elastic modulus and Magness-Taylor value. Similar results were also found with peaches.

Delwiche (1986) studied the relative sensitivity of the frequency spectra to changes in the elastic modulus by modeling the impacts of fruit with the Hertz contact theory developed by Timoshenko and Goodier (1951). Delwiche found that the frequency band between 250 and 340 Hz was the most sensitive to impact velocity and the elastic modulus. He also found that if the impact velocity was held constant, the response for a given frequency can provide a threshold effect for the elastic modulus (the frequency component is very low until the elastic modulus reaches a given value and then becomes large).

The use of System Science parameter identification techniques may also be useful in the analysis of impacts; although not used much in the past. For use in control systems, Rao et al. (1982) applied a method using Poisson moment functions (PMF), which are defined in Equation [3.10], to the identification of parameters in a continuous dynamic system as defined in Equation [3.11]. Rao et al. used a series of analog Poisson filters and a microprocessor for the identification of parameters ($a_{0,1}$, $a_{1,0}$, $a_{1,1}$, $b_{1,0}$, $b_{1,1}$).

$$\left\{ M_K [\, f(t) \,] \right\}_{t_o} \equiv \int_0^{t_o} f(t)\, p_K(t_o - t)\, dt \qquad [3.10]$$

$$\text{order} = K = 0,\ 1,\ 2,\ \ldots$$

where:

$$p_K(t_o) \equiv t_o^K\, e^{-\lambda t_o}/K! \quad , \quad \lambda = \text{constant}$$

$$(1 + a_{0,1}\, t)\frac{d\, f(t)}{dt} + (a_{1,0} + a_{1,1}\, t)\, f(t) = (b_{1,0} + b_{1,1}\, t)\, r(t) \qquad [3.11]$$

By using various properties of the PMF's, a set of simultaneous equations was written and used to find the unknowns in Equation [3.11] without taking noise-prone derivatives. The system parameters can be solved for a single instant of time by using many PMF stages, or can be solved over a period of time by using many samples and a few PMF stages. The initial conditions can also be treated as unknowns and calculated. Rao found two problems with the PMF method, and both problems were related to the multiplexed A/D converters. One problem was related to non-synchronized samples, while the other problem was the low resolution of 8-bit A/D converters when applied to high order PMF's.

3.2 Data Analysis Software

3.2.1 Overview of TESTSYS Program

TESTSYS was developed in Pascal to run on an IBM (or IBM-compatible) personal computer in a MS-DOS environment and to directly analyze IS-formatted data files. TESTSYS also has graphics capabilities which allows the plotting of both raw and processed data on the monitor screen if graphics hardware is present (the graphs can be sent to a printer using the IBM print screen command). TESTSYS is made up of a number of subroutines which can be called from the main program menu. Some of these subroutines are themselves menus. Figure 3.1 shows the menu structure.

In order to avoid the memory limitations associated with personal computers, all of the data are stored in files and read into memory when needed with the results being written back into a file. TESTSYS generates four different types of data files which include: XYZ files, a TABLE file, plot files, and result-listing files. A XYZ file contains a record (each record has a X, Y and Z field) for each vector sample and has no delimiters to separate impacts. Many of the analysis routines generate XYZ

files in which to store intermediate processed data. The TABLE file is also a file of records, but contains the offset information needed in order to find specific impacts within the XYZ file. It also contains impact characteristics such as peak values, peak offsets, areas, time of impact occurrence, etc.. The plot files store the horizontal and vertical coordinates (in binary format) needed to plot the data on the screen. The fourth type of file generated by TESTSYS are text files containing the analysis results in tabular format which may be displayed on the screen or printed.

TESTSYS also has a configuration file and scale calibration factor files. The configuration file is used to set defaults and customize TESTSYS for a specific hardware configuration. However, there is still a need for two versions of the program; one for the IBM graphics adaptor and one for the Hercules graphic adaptor.

3.2.2 Analysis Routines

The first step in analyzing IS data is to read a hexadecimal formatted IS file into TESTSYS and generate the XYZ and TABLE files to be used by the analysis routines. The data may then be analyzed automatically to find the most commonly desired types of information or may be analyzed one step at a time for custom types of information through the auxiliary menu. The automatic analysis procedure

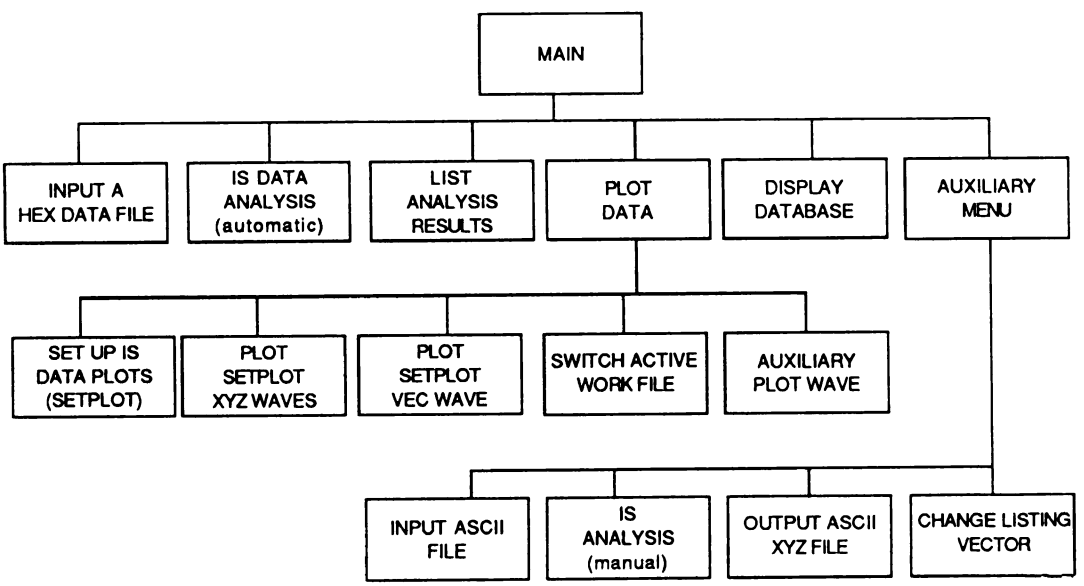

Figure 3.1. Menu structure of TESTSYS.

executes the following routines in the order listed: CONCATIMPACT, RECOVERFILTER, PEAK, ROTATE, CALCVELOCITY, VPEAK, and MAXDROPHT.

HEXINPUT is the routine used to generate XYZ and TABLE files from an IS-formatted file (Figure 2.8). The XYZ file is also scaled by a calibration factor during creation. Besides file creation, HEXINPUT is responsible for initializing some of the program parameters.

HEXINPUT provides the user with four different scaling options: use the scale factor in the data file header, use a scale factor parameter file which contains six multiplication factors (a different factor for positive and negative directions), use a scale factor parameter file which contains three bias factors and three multiplication factors, or do no data scaling at all. The desired option is selected by entering INTERNAL, NONE or a valid scale factor file name when prompted for a scale factor file name. The first number in the parameter file will be used to decide which of the two parameter file options will be used.

When the data file header scale factor is used, the internal scale factor is derived from Equation [3.12]. GScale is a three byte word located at 0DH in the HEX data file.

$$\text{Internal scale factor} = \text{GScale} * 10^{-4} \qquad [3.12]$$

The IS unit described in this thesis was calibrated to use a parameter file containing three bias factors and three multiplication factors.

CONCATIMPACT compares the time between impacts and joins the impacts together if only one data point is missing between them. While joining the impacts together, an extra point is added between the impacts by averaging the two end points next to the gap. For each concatation, a record is removed from the TABLE file and an interpolated data record is added to the XYZ file. The TABLE file record for the original impact must also be updated to reflect the additional data points. No additional files are generated by this routine, however the old files are modified.

RECOVERFILTER implements a pre-emphasis digital filter to recover the low frequencies attenuated by the piezoelectric accelerometer and the AC coupling circuits in the IS. Equation [3.13] is used to achieve the compensation filter.

$$Y[k] = (1/a) * X[k] - X[k-1] + Y[k-1] \qquad [3.13]$$

where:

$X[k]$ = input data, $Y[k]$ = output data

$a = 1 / (1 + w_c*T)$

w_c = cutoff freq., T = sample period

Two Rad/s was used as the cutoff frequency, but may be changed by the configuration file. This subroutine modifies the original XYZ file. Equation [3.13] is replicated three times; once for each axis.

PEAK is used to find the peak acceleration values and the offset times (time between the start of the impact and the peak) associated with the peak values. The peak acceleration is determined from the vector sum of the acceleration data and is found by simply searching the data for the maximum vector sum value and recording it along with it's offset (number of samples) to the TABLE file. This is repeated for each impact in the data set.

ROTATE is used to rotate the coordinate system for each impact such that the peak acceleration occurs on the new "x-axis" with the values on the other axis being zero at the peak. The coordinate rotation is done by finding the cosines of the peak acceleration vector and using them to form a rotation matrix which is multiplied by all of the sample vectors from the impact. This procedure is repeated for all of the impacts in the data set. The offset of the peak acceleration sample is found in the TABLE file and the cosines of the peak value are stored in the TABLE file after being calculated. ROTATE also produces a new XYZ file.

CALCVELOCITY is used to integrate an acceleration XYZ file by the trapezoidal method and create a new XYZ file containing the integrated values. Since the original XYZ file contained acceleration, the integrated XYZ file will contain velocity (and in the rotated coordinate system if called from the automatic analysis procedure). Each axis is integrated separately and stored separately in the new XYZ

file. Zero is used as the initial condition in Equation [3.14] which shows the trapazoidal integration method.

$$y[i] = y[i-1] + ((x[i-1]+x[i]) / (\text{sample rate}*2)) \quad [3.14]$$

where:

x[i] = input data

y[i] = integrated data

VPEAK is used to find the overall velocity change during the impacts and must be called after ROTATE and CALCVELOCITY. The overall velocity change is found by scanning the X-axis of the velocity file for the maximum value which also is a zero crossing in the acceleration data and finding the vector sum at that point. The offset of the peak velocity is used as the impact duration since it is a zero crossing for acceleration. The overall velocity change and offset of the point are both stored in the TABLE file.

MAXDROPHT uses the peak velocity found by VPEAK to calculate the maximum possible drop height by assuming that there is no rebound. The velocity calculated by VPEAK is the total velocity change (impact velocity plus rebound velocity) during the impact; therefore by assuming that the rebound velocity equal zero, the peak velocity then equals the impact velocity. Equation [3.15], which is used to calculate the maximum drop height, also assumes free fall under the influence of gravity.

$$\text{MaxDrop} := \text{sqr}(\text{Peak Velocity}) / (2 * a) \quad [3.15]$$

where:

a = acceleration due to gravity

3.2.3 Utility Routines

LISTTABLE is used to write the analysis results contained in the TABLE file to a logical DOS file which may include CON (screen) or PRN (printer). The text output from LISTTABLE is formatted to fit on a 66 line page unless CON is used as the output file; in which case the output is formatted to fit on a 24 line screen. Depending on the configuration, the following information can be listed by LISTTABLE: time of occurrence, impact duration, number of sample points in the impact, peak

acceleration, offset of the peak sample, peak velocity, offset of peak velocity, the cosines from the peak acceleration vector, and the maximum possible impact velocity (assuming no rebound). Usually only part of the above information is listed due to the limited number of columns on the screen or paper. The TESTSYS configuration file contains the default listing options, however the listing options can be changed while running the program. Figure 3.2 shows an example listing.

PLOTWAVE is used to present the IS data in a graphical format on the computer screen. PLOTWAVE has a menu which contains the following: Setup IS Data Plots, Plot XYZ Waves, Plot VEC Wave, switch the active XYZ file, and Auxiliary Plot Menu. The "Setup IS Data Plots" procedure

Created: 5/ 1/87 14:26:50 a:dp05.hex

Time Sec.	Duration msec.	No Pt #	Peak g	VPeak m/s	MaxDrop m
23.213	6.6	20	29.3	1.37816	0.097
23.338	5.0	15	16.1	0.63863	0.021
31.186	7.0	21	27.7	1.29735	0.086
31.312	6.3	19	14.5	0.66408	0.022
31.392	0.3	1	9.9	0.00000	0.000
37.290	6.6	20	25.7	1.13273	0.065
37.419	4.3	13	11.0	0.33878	0.006
42.798	6.0	18	32.3	1.48222	0.112
42.922	3.6	12	15.3	0.48465	0.012
49.357	7.3	22	32.6	1.69677	0.147
49.486	6.0	18	18.8	0.86584	0.038
49.564	1.0	3	12.0	0.07830	0.000
49.567	1.3	4	12.0	0.12113	0.001
53.854	5.6	18	30.4	1.40338	0.100
53.981	0.3	1	16.0	0.00000	0.000
53.982	1.3	4	18.5	0.18122	0.002
58.436	7.3	22	33.3	1.71886	0.151
58.561	5.6	19	19.5	0.94358	0.045
58.638	3.0	9	13.6	0.39311	0.008
62.865	7.3	22	31.9	1.57056	0.126
62.991	6.3	19	17.9	0.80822	0.033
63.069	0.3	1	11.1	0.00000	0.000
67.264	6.3	19	25.5	1.13361	0.065
67.390	4.3	13	11.6	0.39545	0.008
71.570	5.0	16	25.7	0.94041	0.045
71.696	2.3	7	11.7	0.20806	0.002

Figure 3.2. Sample listing from TESTSYS.

generates four plot files (X.BIN, Y.BIN, Z.BIN and V.BIN) which when plotted show the impacts in real time with the time axis labeled in seconds and with zero being the time at which the IS data file was created. The Setup procedure allows the user to specify the real start time and duration of the plots, in order to focus on small segments of the data if desired. The Setup procedure also allows the user to scan the data for the next impact from a starting point. All timing information about the impacts is obtained from the TABLE file. The Plot XYZ option splits the screen into three sections and plots the x,y and z data in the three sections. The Plot VEC option plots the vector sum data on the screen. An example XYZ plot is shown in Figure 3.3. The switch active XYZ file option activates the subroutine SWITCH. The Auxiliary Plot Wave option is being used for developmental work.

The subroutine SWITCH is used to change the active XYZ file since there may be more than one XYZ file. Any of the intermediate XYZ files can be plotted by using this subroutine to make them active. SWITCH will list the allowable XYZ files when executed and a file from this list must be selected.

The subroutine OASCII1 is in the file utility menu and is used to convert a binary plot file generated by Set Plot to an ASCII text file which can be read by other plotting packages. This may be desirable since TESTSYS does not drive pen plotters or laser printers.

SHOWDATABASE is used to display general parameters from the IS file being worked on. Some of the parameters displayed include: sampling rate, threshold values, scale factors, the file name of the input file, etc..

3.3 Analysis of Controlled Impacts

A set of six controlled impact tests were performed to judge the performance of the IS and analysis software. The tests were done at three drop heights (0.05 m, 0.10 m, and 0.20 m) onto two different pads resting on a concrete floor. One pad was a 6.35 mm (1/4 in) thick piece of foam rubber with skin (the same type of padding used in commercial packing lines) mounted to a 19.05 mm (3/4 in) thick piece of plywood. The other pad was a 5 ms duration elastomer which is used by packaging engineers for impact testing. For the tests, the IS was released by hand from a height measured with a wooden

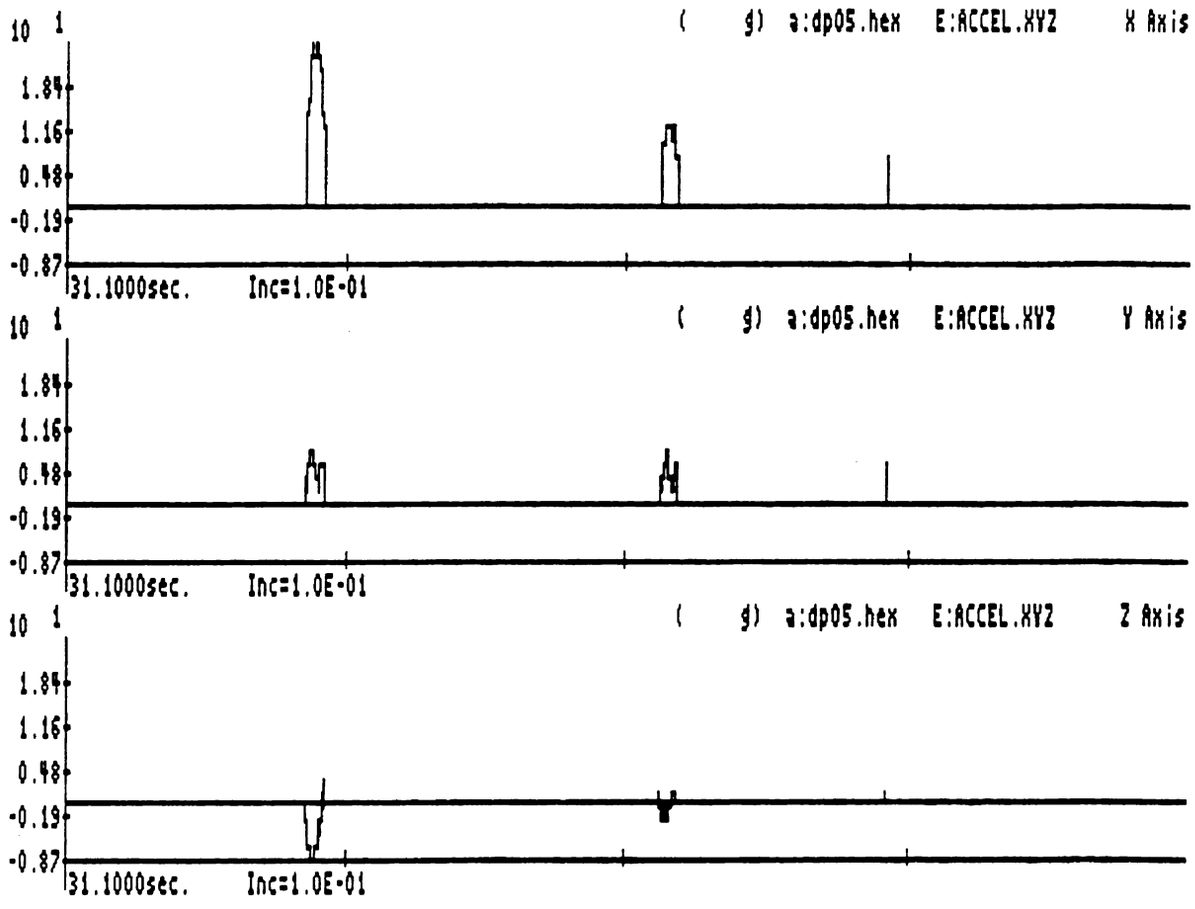

Figure 3.3. Sample XYZ plot from TESTSYS.

gauge block, which contributed an estimated error of ±5 mm. After the main impact, the IS was allowed to bounce until it came to rest; thereby making it possible to calculate the coefficient of restitution based on the time between impacts. Ten drops were made for each of the six tests with the point of impact occurring on different sides of the IS for each drop. The IS threshold setting and sampling rate were 8 g and 3019 Hz, respectively.

The results from the drop tests, which are listed in Tables 3.1 to 3.6, were compiled by using TESTSYS and another program that further analyzed the output listings from TESTSYS. Two of the impacts recorded are shown in Figures 3.4 and 3.5. The true impact velocities for the 0.05, 0.10, and 0.20 meter drops are 0.990, 1.40, and 1.98 m/s, respectively as calculated from the free fall Equation [3.16]. The coefficients of restitution, listed in Tables 3.1 to 3.6, were calculated using Equation [3.17] which incorporates the time between bounces of the IS and the true impact velocity. The predicted impact velocity in Equation [3.18] was obtained from the total velocity change (from TESTSYS) and from the coefficient of restitution.

$$\text{true impact velocity} = \text{sqrt}(2 * a * \text{drop ht.}) \qquad [3.16]$$

where:

a = acceleration due to gravity

$$\text{coeff. rest.} = (a * (\text{delta}/2)) / \text{true impact velocity} \qquad [3.17]$$

where:

delta = time between the 1 st. and 2nd. bounces

$$\text{predicted impact velocity} = \frac{\text{total velocity change}}{(1 + \text{coeff. rest.})} \qquad [3.18]$$

Table 3.7 further summarizes the results from the drop tests by listing the errors in the predicted impact velocities and the average coefficients of restitution. It should be noted that the actual error and percent error in predicted impact velocity tends to decrease as the drop height increases. This may be due to the 2 g resolution of the acceleration values or due to the thresholding which causes the leading

Table 3.1. Results from dropping the IS onto a foam rubber pad from 0.05 m causing an impact velocity of 0.99 m/s.

Drop No.	Duration (ms)	Peak (g)	Total Vel. Change (m/s)	Coeff. of Rest.	Predicted impact Vel. (m/s)
1	7.3	40.4	1.70	0.882	0.90
2	6.3	30.8	1.36	0.872	0.73
3	5.6	27.9	1.02	0.877	0.54
4	6.3	26.3	1.07	0.872	0.57
5	6.3	33.8	1.36	0.872	0.73
6	7.3	33.7	1.66	0.857	0.90
7	7.9	37.7	1.77	0.857	0.95
8	8.6	36.2	1.82	0.867	0.98
9	7.6	37.7	1.69	0.847	0.91
10	6.3	30.0	1.21	0.872	0.65
Mean				0.867	0.79
Standard Deviation				0.011	0.15

Table 3.2. Results from dropping the IS onto a foam rubber pad from 0.10 m causing an impact velocity of 1.40 m/s.

Drop No.	Duration (ms)	Peak (g)	Total Vel. Change (m/s)	Coeff. of Rest.	Predicted impact Vel. (m/s)
1	5.6	91.3	2.35	0.812	1.30
2	6.3	88.1	1.97	0.774	1.11
3	5.3	81.7	2.14	0.788	1.20
4	6.3	93.9	2.50	0.819	1.37
5	6.3	79.0	2.30	0.816	1.27
6	5.6	100.2	2.49	0.812	1.38
7	6.0	98.7	2.45	0.812	1.35
8	5.6	87.9	2.26	0.812	1.24
9	6.6	78.6	2.29	0.809	1.27
10	5.0	100.6	2.13	0.819	1.17
Mean				0.808	1.27
Standard Deviation				0.014	0.08

Table 3.3. Results from dropping the IS onto a foam rubber pad from 0.20 m causing an impact velocity of 1.98 m/s.

Drop No.	Duration (msec.)	Peak (g)	Total Vel. Change (m/s)	Coeff. of Rest.	Predicted impact Vel. (m/s)
1	5.3	192.6	3.36	0.733	1.94
2	5.6	203.8	3.31	0.726	1.92
3	5.0	178.4	2.99	0.681	1.78
4	5.0	137.3	2.67	0.723	1.55
5	5.0	209.3	3.46	0.726	2.00
6	4.3	202.1	3.26	0.730	1.88
7	4.6	231.9	3.48	0.750	1.99
8	5.0	190.7	3.30	0.733	1.91
9	6.3	131.0	3.16	0.706	1.85
10	4.3	158.7	2.85	0.716	1.66
Mean				0.722	1.85
Standard Deviation				0.018	0.14

Table 3.4. Results from dropping the IS onto a 5 ms duration elastomer pad from 0.05 m causing an impact velocity of 0.99 m/s.

Drop No.	Duration (msec.)	Peak (g)	Total Vel. Change (m/s)	Coeff. of Rest.	Predicted impact Vel. (m/s)
1	6.6	29.3	1.31	0.619	0.81
2	7.0	27.7	1.30	0.624	0.80
3	6.6	25.7	1.13	0.639	0.69
4	6.0	32.3	1.31	0.614	0.81
5	7.3	32.6	1.70	0.639	1.04
6	6.0	30.4	1.40	0.634	0.86
7	7.3	33.3	1.68	0.619	1.04
8	7.3	31.9	1.57	0.624	0.97
9	6.3	25.5	1.12	0.624	0.69
10	5.3	25.7	0.94	0.624	0.58
Mean				0.626	0.83
Standard Deviation				0.008	0.14

Table 3.5. Results from dropping the IS onto a 5 ms duration elastomer pad from 0.10 m causing an impact velocity of 1.40 m/s.

Drop No.	Duration (ms)	Peak (g)	Total Vel. Change (m/s)	Coeff. of Rest.	Predicted impact Vel. (m/s)
1	7.0	48.8	2.21	0.613	1.37
2	7.0	42.3	1.99	0.616	1.23
3	7.3	44.5	2.03	0.616	1.26
4	7.0	45.0	2.08	0.616	1.29
5	7.9	49.9	2.42	0.613	1.50
6	7.3	44.5	2.27	0.609	1.41
7	7.9	44.1	2.21	0.609	1.37
8	7.0	45.4	2.22	0.609	1.38
9	7.9	42.8	2.08	0.602	1.30
10	6.6	40.2	1.74	0.613	1.08
Mean				0.612	1.32
Standard Deviation				0.004	0.11

Table 3.6. Results from dropping the IS onto a 5 ms duration elastomer pad from 0.20 m causing an impact velocity of 1.98 m/s.

Drop No.	Duration (msec.)	Peak (g)	Total Vel. Change (m/s)	Coeff. of Rest.	Predicted impact Vel. (m/s)
1	7.0	70.9	3.08	0.597	1.93
2	7.0	60.2	2.66	0.597	1.67
3	6.6	65.4	2.96	0.602	1.85
4	6.6	66.4	2.78	0.602	1.74
5	7.6	74.1	3.43	0.599	2.14
6	7.9	70.7	3.23	0.599	2.02
7	7.3	61.6	2.85	0.597	1.78
8	7.0	67.7	2.97	0.594	1.86
9	7.3	59.3	2.67	0.592	1.68
10	7.6	69.7	3.36	0.599	2.10
Mean				0.598	1.88
Standard Deviation				0.003	0.16

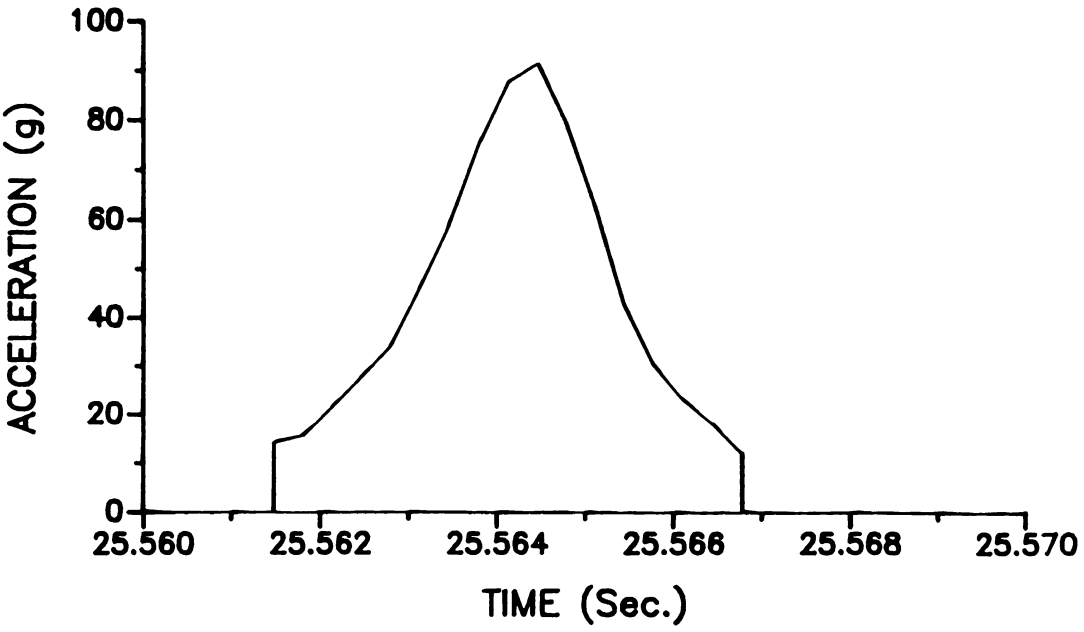

Figure 3.4. The vector sum of an impact onto a foam rubber pad from 0.10m.

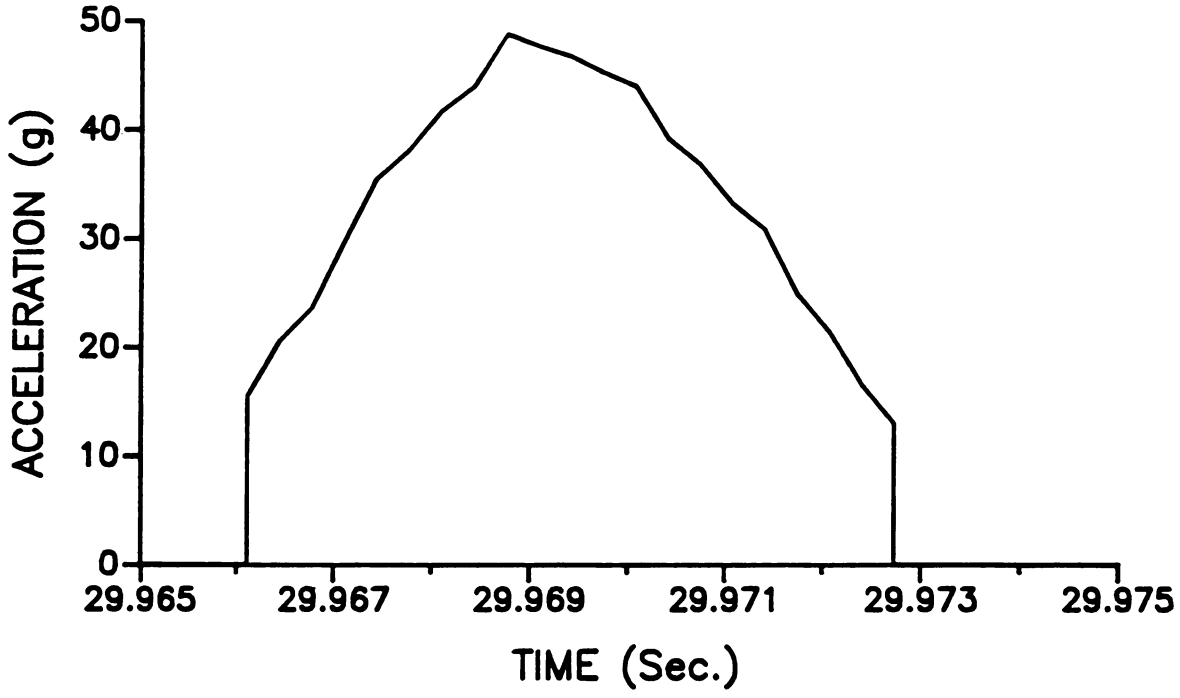

Figure 3.5. The vector sum of an impact onto the elastomer pad from 0.10m.

Table 3.7. A summary of results from tables 3.1 to 3.6 along with error information.

	Test	Coeff. of Rest.	True Impact Velocity (m/s)	Predicted Impact Vel. (m/s)	Actual Error (m/s)	% Error
Foam						
	0.05m	0.87	0.99	0.79	-0.20	-20
	0.10m	0.81	1.40	1.27	-0.13	- 9
	0.20m	0.72	1.98	1.85	-0.13	- 7
Elastomer						
	0.05m	0.63	0.99	0.83	-0.16	-16
	0.10m	0.61	1.40	1.32	-0.08	- 6
	0.20m	0.60	1.98	1.88	-0.10	- 5

and trailing edges of the impact to be missed. The leading and trailing edge loss will be most significant in small impacts. The errors for the elastomer pad also tend to be less then the errors for the foam pad.

The tests also verified that the coefficients of restitution are not constants but vary with impact velocity, decreasing as the impact velocity increases. Although the coefficients of restitution could be calculated for the above tests, they generally cannot be calculated from the IS data, since the drop height and the conditions acting on the IS between impacts are not known.

3.4 Packing Line Tests

3.4.1 Description of the Packing Line and Procedures

Survey tests using the IS were made on two Michigan packing lines which will be denoted as "line #1" and "line #2". Because of the large IS, a few sections of both packing lines could not be utilized in the survey tests. Line #1 was divided into three sections; submergible dump tank to the electronic sizer (excluding most of the electronic sizer), electronic sizer to bagger, and bagger to shipping carton stage. The survey tests for line #2 were less extensive then for line #1, covering only the section of line between the electronic sizer and shipping carton stage.

The following is a brief description of packing line #1. The first component in packing line #1 is a submergible dumper which is used to float apples out of bulk boxes. The apples then float to point A (see Figure 3.6) where a roller conveyor lifts the apples out of the water and transfers them onto an

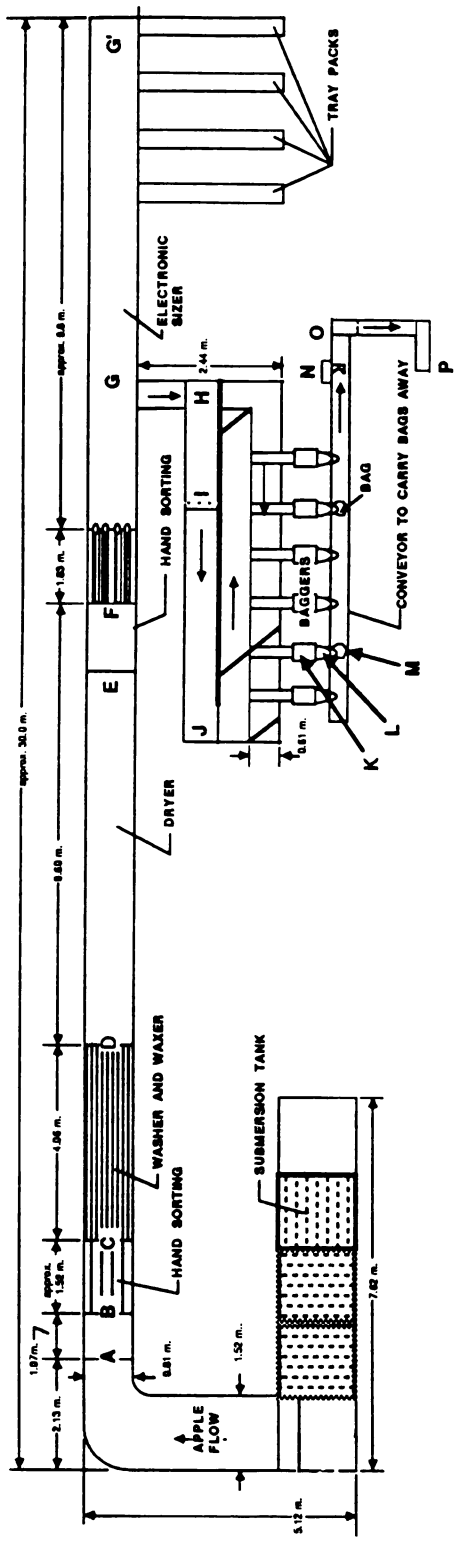

Figure 3.6. Layout of packing line #1.

inspection conveyor, point B. From point B the apples travel to point C where they enter the washer/waxer, which is divided into three stages: washing, absorber roller drying, and waxing. The apples are moved through the washer/waxer on 76.2 mm (3 in) diameter brushes with axes of rotation perpendicular to the direction of travel. At the end of the washer/waxer, point D, the apples enter a heated drying tunnel which dries the wax. The apples travel through the tunnel on 57.2 mm (2.25 in) diameter aluminum rollers attached to a conveyor. Directly after the drying tunnel, but on the same conveyor, is an inspection station from where the apples descend 177.8 mm (7 in) to a four channel singulater (point F), a part of the electronic sizer. The singulater then places the apples into the sizer's cups slightly beyond point F, from where they travel to the various drop points, such as at point G. At the drop point, the cup flips open, dropping the apples 254 mm (10 in) to a cross conveyor belt. All fruit using the point G drop out are eventually transferred to the bidirectional belt accumulator at point H via the G-H conveyor. The bagging units pull apples off the bidirectional belts by using a narrow perpendicular belt overlapping the outside bidirectional belt. At the end of the perpendicular belt (point K), is a double pair of spiral rolls used to feed the fruit onto the scale (point L). The scale empties into a bag after a preset weight is reached. The full bags then move on a conveyor from the bagger, point M, to a taping station at point N where they are taped (bag closing) and placed back onto the conveyor. At point O the bags start up an incline to be placed in shipping cartons at point P.

Described in this paragraph is the section of packing line #2 used for the survey tests, mainly the bagging operation. Upon being dropped from the electronic sizer, the apples fall onto a cross conveyor belt which carries them to point B (see Figure 3.7) where they enter a bidirectional belt accumulator which feed the baggers. The belt closest to the baggers, has 12.7 mm (1/2 in) diameter rods placed above the belt at an angle to direct apples into the bagging units (point C). After leaving the bidirectional belts, the apples transfer directly onto a double pair of spiral rolls which feed the scale pan (point D). When the scale reads the preset weight, the apples are dumped into a bag. After being bagged the apples travel to the taping station at point F where the bags are taped shut. From the taper, the bags are placed

back on a conveyor belt and travel up an incline to a rotating table at point G from where they are packed into shipping cartons at point H.

For the tests at both packing lines, a workstation was setup in a room adjacent to the packing line in order initialize the IS and upload the recorded data. Initialization involved setting the sampling rate to 3019 Hz, setting the threshold to either 6 or 8 g. and entering the current date and time. At packing line #1 all runs were made with a 6 g threshold, except for the first which was made with a 8 g. threshold. Two runs were made at packing line #2, with the first having a 6 g threshold and the second a 8 g threshold. After initialization, the IS was carried to the line, run through a section of line, and then carried back to the workstation for data transferral. Two runs were made for each section of line tested.

During the tests, both a VCR and note paper were used to document the position of the IS on the packing line verses the time into the test. This was necessary since the IS only keeps track of time.

3.4.2 Results

The six tests made at packing line #1 will be presented first, followed by the results from the two tests made at packing line #2. In the following discussion, an impact of less than 9 g will be considered a low level impact and an impact with a duration of less than 2/3 ms will be considered a short impact.

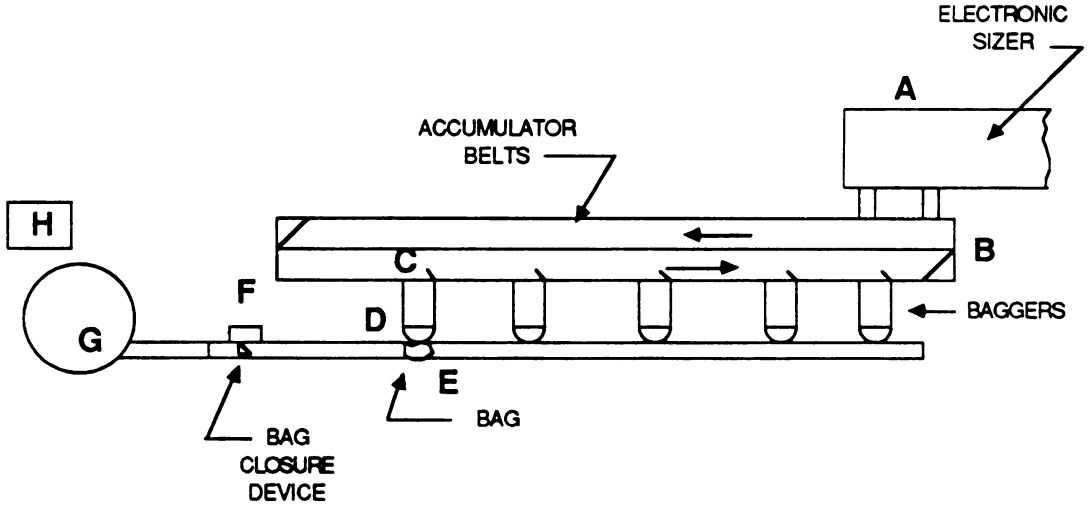

Figure 3.7. Layout of packing line #2.

Impacts with a total change in velocity of less than 0.165 m/s will be considered insignificant and will not be mentioned in most of the results.

Results From Packing Line #1

Test #1:

This test was run on the first section of packing line #1, starting at the first inspection station located between points B and C, and ending just before the electronic sizer located at point F. The most significant impacts (having a total velocity change 0.145 m/s) from test #1 are listed in Table 3.8.

The first three impacts in Table 3.8 were due to the transfer to the washer and waxer at point C, with the primary impact (impact at 210.430 s) having a magnitude of 17.2 g and a duration of 4.3 ms.

The last four impacts listed in Table 3.8, occurred when the IS transferred from the second inspection station to the singulater at point F, and are shown in Figure 3.8. The four impacts decreased in peak magnitude, and had an approximate separation of 0.06 s.

The maximum possible drop height for test #1 was 0.034 m and occured when the IS transferred to the singulater at point F. Most of the maximum possible drop heights for test #1 were less than 0.01 m.

Test #2:

This test covered the same section of line as test #1, with the addition of the transfer onto the hand sorting conveyor at point B, and a ride on the electronic sizer conveyor from point G to G'. The threshold setting for this test was 6 g. Figure 3.9 is a plot of the results from test #2 and Table 3.9 lists all of the significant impacts for the test.

The impacts at 140.850 s and 170.939 s will be ignored since one occurred before the IS was placed on the packing line and the other occurred when the IS was accidentally dropped into the dumper tank. The first legitimate impact occurred at 189.182 s when the IS transferred to the first inspection conveyor at point B. This impact is shown in Figure 3.10.

Table 3.8. Results from test #1 at packing line #1.

Time s	Duration msec.	No. Pt #	Peak g	Peak Vel. m/s	MaxDrop m	location
210.430	4.3	13	17.2	0.534	0.015	C
210.436	6.6	20	14.4	0.771	0.030	C
210.686	2.3	7	10.4	0.182	0.002	C
498.586	4.3	13	30.4	0.821	0.034	F
498.675	5.0	15	17.0	0.649	0.021	F
498.741	2.6	8	18.7	0.363	0.007	F
498.805	3.6	11	18.8	0.519	0.014	F

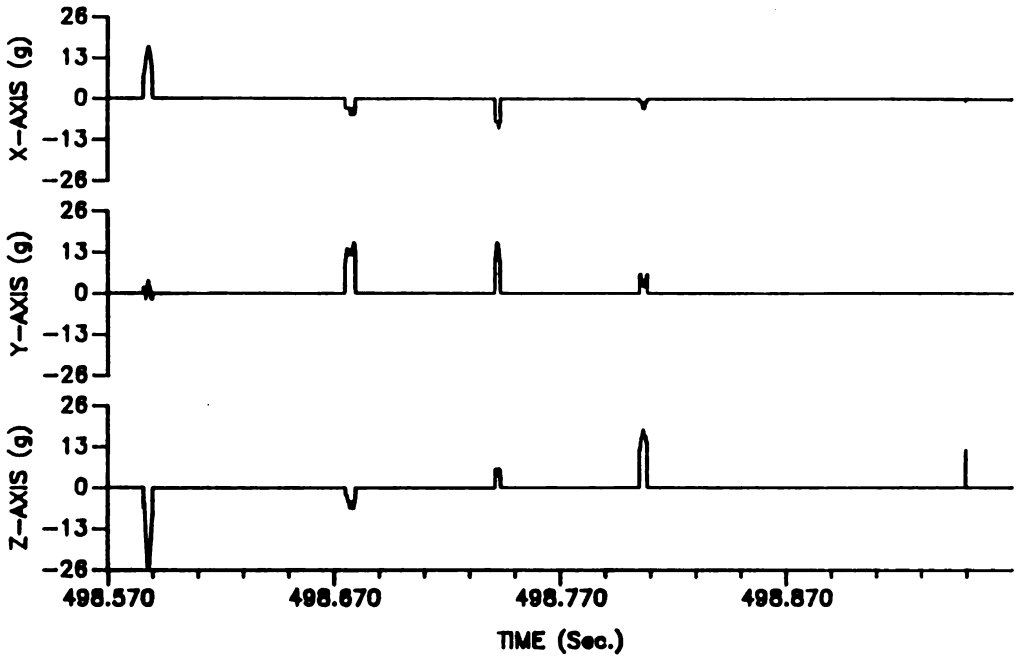

Figure 3.8. Impacts from the IS hitting the metal divides at point F of packing line #1.

Table 3.9. Results from test #2 at packing line #1.

Time s	Duration ms	No. Pt #	Peak g	Peak Vel. m/s	MaxDrop m	Location
140.850	2.0	6	14.9	0.216	0.002	pre-A
170.939	7.3	22	25.5	1.181	0.071	A
189.182	6.0	18	15.8	0.699	0.025	B
508.938	6.0	18	15.0	0.737	0.028	F
509.042	10.9	33	13.4	1.182	0.071	F
509.357	2.0	6	10.3	0.165	0.001	F
509.408	5.0	15	14.8	0.569	0.017	F
509.821	3.6	11	13.9	0.391	0.008	F
510.337	2.3	7	11.4	0.209	0.002	F

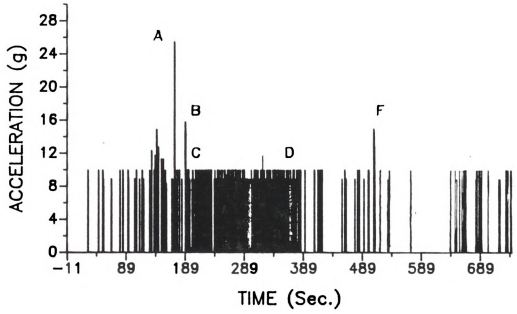

Figure 3.9. Vector sum plot of test #2 on packing line #1.

No large impacts occurred between points B and F, but low level impacts from the washer and waxer can be clearly seen in Figure 3.9. The transfer to the singulater at point F generated the series of six impacts which started at 508.938 s and are listed in Table 3.9. A maximum possible drop height of 0.071 m was also reached at this point.

After picking the IS up at point F, it was set onto the electronic sizer conveyor at point G and traveled the full length of the conveyor to point G'. As shown in Figure 3.9, no high level impacts resulted from the ride.

Test #3:

This test was ran on packing line #1, starting at point G on the cross conveyor below the electronic sizer, and ending just before the bag at point M. The threshold setting for this test was 6 g. Table 3.10 lists all the significant impacts. The first impact listed on Table 3.10 (at 175.055 s) occurred approximately at the time when the IS transferred to the bidirectional belts at point J.

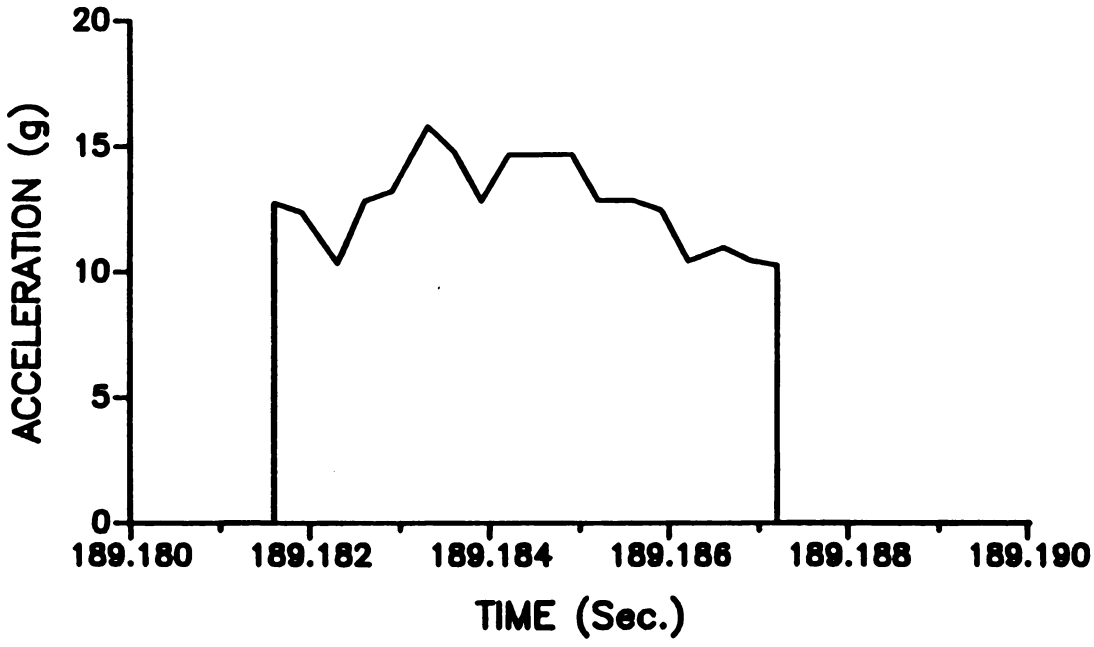

Figure 3.10. An impact resulting from the IS landing on the hand inspection conveyor at point B of packing line #1.

Table 3.10. Results from test #3 at packing line #1.

Time s	Duration ms	No. Pt #	Peak g	Peak Vel. m/s	MaxDrop m	Location
175.055	3.0	9	13.2	0.294	0.004	J
369.470	5.0	15	16.4	0.535	0.015	K
375.848	5.0	15	13.0	0.469	0.011	L
376.491	2.6	8	13.3	0.267	0.004	L
376.705	2.3	7	10.9	0.197	0.002	L

While on the accumulator, a number of low level impacts (approx. 7 g) were recorded due to apples impacting the IS. As listed on Table 3.10, the next significant impact occured at 369.470 s while the IS was on the spiral feed rolls (point K) of the bagger. While on the spiral rolls, there were also several low level impacts (approx. 7 g) not listed in Table 3.10. The last three impacts listed on Table 3.10 occurred when the IS transferred to the scale pan at point L with the primary impact having a magnitude of 13 g and a duration of 5 ms.

The maximum possible drop heights for this test was 0.015 m.

Test #4:

This test was started at point I to avoid an overhead obstruction which had caused a problem in test #3 and then covered the same section of line as test #3. The threshold setting for this test was 6 g. Table 3.11 lists all of the significant impacts (a complete listing is in the appendix) for test #4 while Figure 3.11 shows a plot of the whole test.

The first impact listed on Table 3.11 occurred at approximately the time the IS was transferred to the bidirectional belts at point J. The next nine significant impacts (230.482 s to 247.253 s) were caused by the spiral rolls of the bagger at point K. Figure 3.12 shows these nine impacts along with many other low level impacts which also occurred. The open gaps in the trace at 238 s and 248 s are due to the spiral rolls being stopped temporarily. The last two impacts on Table 3.11 occurred as the IS transferred to the scale at point L.

Table 3.11. Results from test #4 at packing line #1.

Time s	Duration ms	No. Pt #	Peak g	Peak Vel. m/s	MaxDrop m	location
113.140	3.3	10	14.9	0.397	0.008	J
230.482	3.6	11	15.7	0.436	0.010	K
236.433	2.0	6	10.7	0.166	0.001	K
244.946	3.3	10	12.2	0.317	0.005	K
246.339	2.0	6	10.5	0.153	0.001	K
246.348	2.3	7	12.7	0.218	0.002	K
246.418	2.3	7	14.2	0.244	0.003	K
246.426	4.3	13	10.7	0.343	0.006	K
246.801	3.3	10	12.4	0.321	0.005	K
247.253	2.3	7	12.8	0.210	0.002	K
250.958	3.3	10	12.9	0.333	0.006	L
255.518	2.3	7	10.9	0.203	0.002	L

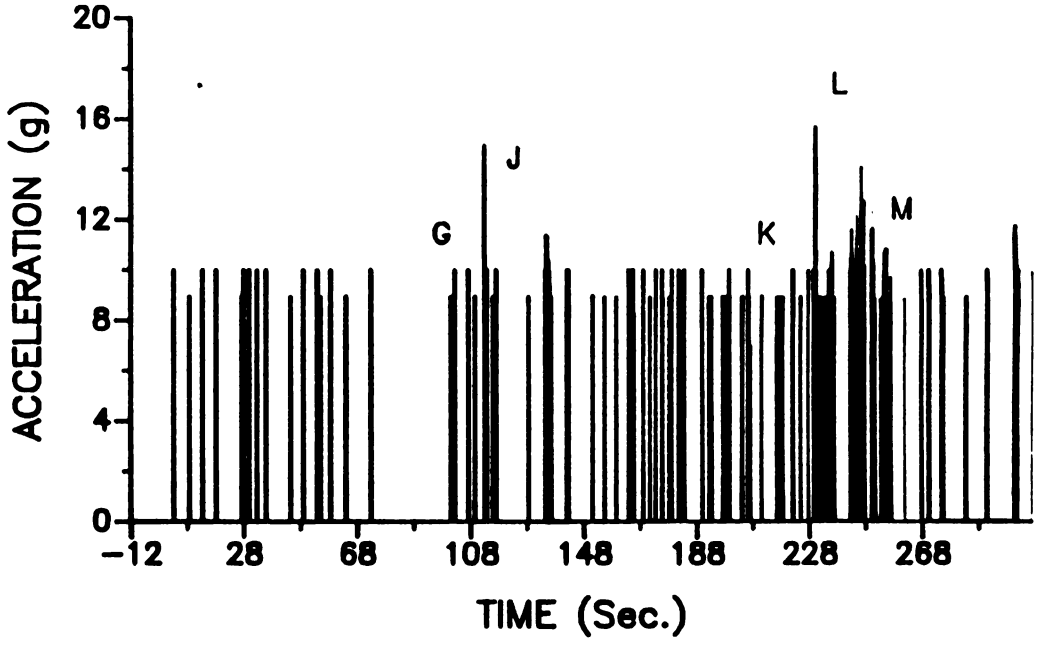

Figure 3.11. Vector sum plot of test #4 on packing line #1 (electronic sizer to the bagger).

The maximum possible drop heights for this test were less than or equal to 0.015 m.

Test #5:

This test started with exposure to electrical noise from such sources as motors, control boxes and solenoids. Following the noise exposure, the IS was put in a bag of apples and placed on the packing line at point M just beyond the bagger. The test ended after the bag was placed into the shipping carton at point P. This test was ran with a 6 g threshold and the significant impacts are listed in Table 3.12.

Noise from the electrical sources was detected but none of the levels were significant and thus not recorded in Table 3.12. The first six impacts (327.060 s to 332.854 s) listed in Table 3.12 were related to the bag being taped at point N with the primary impact reaching a peak of 64.8 g. Figure 3.13 shows that these impacts were from several directions, therefore possibly involving more than one surface. This bag taping operation also produced an impact with a maximum possible drop height of 0.157 m.

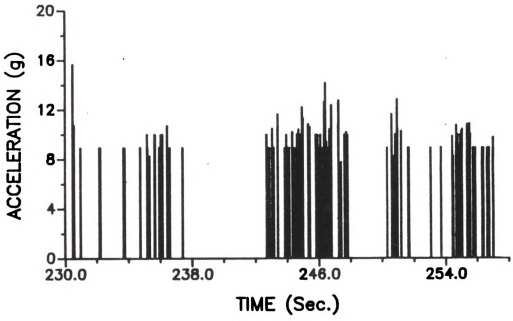

Figure 3.12. A vector sum plot of the impacts which occured while the IS was on the spiral feed rolls at point K.

Table 3.12. Results from test #5 at packing line #1.

Time s	Duration ms	No. Pt #	Peak g	Peak Vel. m/s	MaxDrop m	Location
327.060	4.3	13	64.8	1.757	0.157	N
327.174	5.3	16	18.3	0.651	0.022	N
329.880	2.0	6	27.5	0.333	0.006	N
330.092	4.0	12	19.2	0.529	0.014	N
330.137	2.0	6	10.7	0.158	0.001	N
332.854	3.0	9	18.3	0.407	0.008	N
340.740	1.7	5	60.9	0.543	0.015	O
340.808	4.3	13	19.0	0.582	0.017	O
342.383	4.0	12	11.9	0.385	0.008	post O
342.389	2.3	7	11.8	0.217	0.002	post O
342.428	1.7	5	11.8	0.151	0.001	post O
342.431	2.3	7	12.6	0.214	0.002	post O
342.441	2.0	6	11.8	0.178	0.002	post O
354.113	1.7	5	11.8	0.146	0.001	L
354.126	2.0	6	11.8	0.176	0.002	L

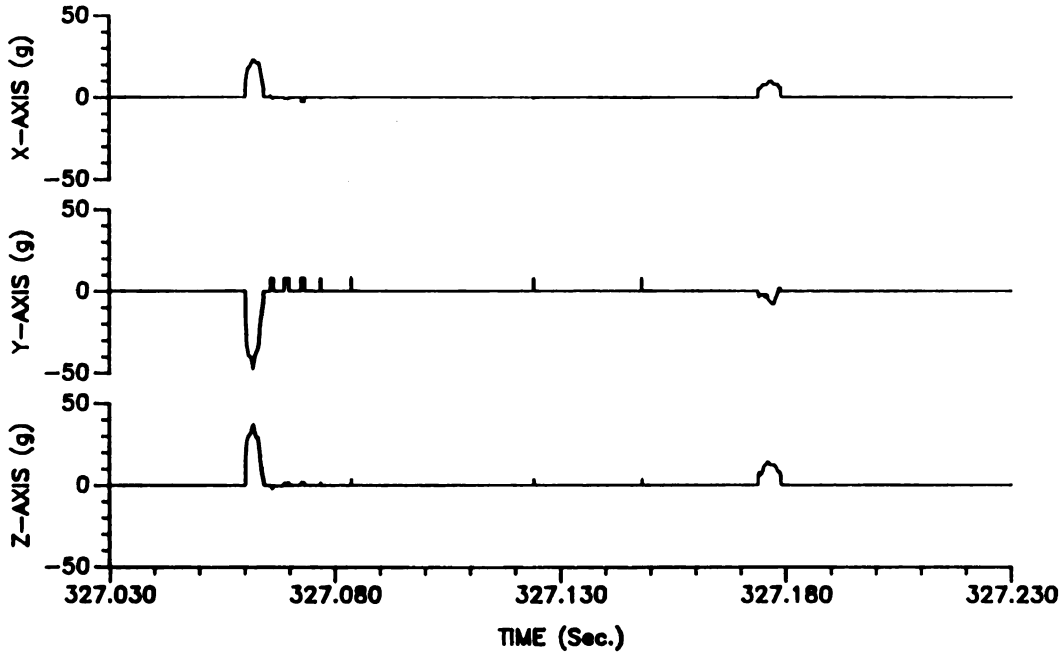

Figure 3.13. Impacts from the bag being taped at point N on packing line #1.

The next two impacts (340.740 s and 340.808 s) listed in Table 3.12 were due to the IS transferring conveyors at point O and are shown in Figure 3.14 along with some smaller impacts which also resulted from the transfer. Some impacts were also recorded from the bag tumbling backwards as it was carried up the conveyor located between points O and P. These are the impacts which occurred between 342.383 s and 342.441 s. These impacts resulted in what appears as vibration in the IS as is shown in Figures 3.15.a and 3.15.b. The final two significant impacts occurred when the bag containing the IS was placed into the shipping carton at point L.

Test #6:

This last test for packing line #1 covered the same section as test #5 with exception that no noise was deliberately recorded. A 6 g threshold was also used in this test and the results are plotted in Figure 3.16 and the most significant impacts are listed in Table 3.13.

The first two impacts in Table 3.13 were due to the bag taping operation at point N. The impact at 81.064 s is shown in Figure 3.17. The bag taping operation again caused an impact with a large maxi-

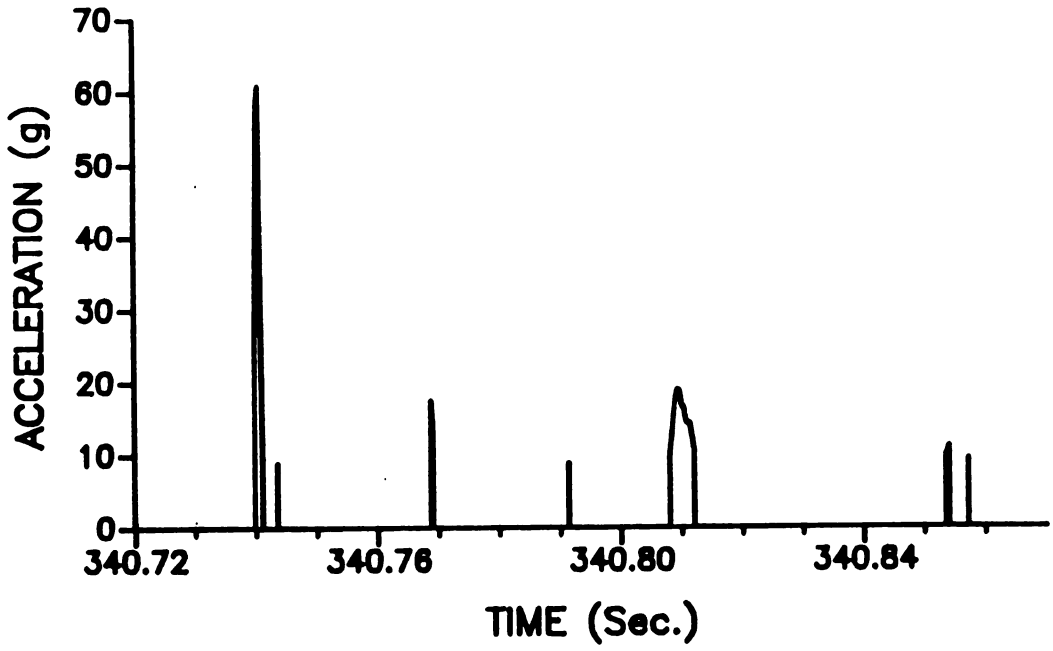

Figure 3.14. A vector sum plot of the impacts at point O on packing line #1.

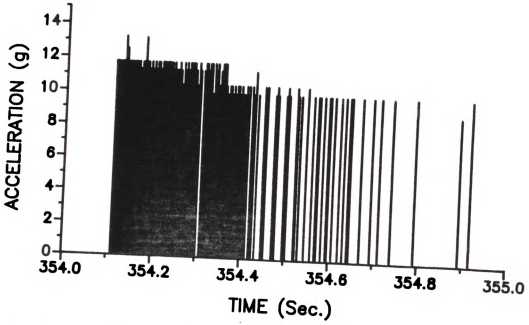

Figure 3.15.a. A plot showing IS vibration which occurred between points O and P.

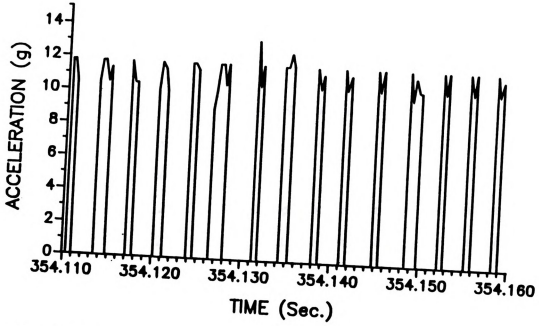

Figure 3.15.b. A section of figure 3.15.b at a finer time scale.

Table 3.13. Results from test #6 at packing line #1.

Time s	Duration ms	No. Pt #	Peak g	Peak Vel. m/s	MaxDrop m	Location
81.064	3.6	11	30.1	0.731	0.027	N
83.852	4.0	12	14.0	0.444	0.010	N
93.736	1.7	5	25.3	0.251	0.003	O
93.947	2.6	8	17.7	0.314	0.005	O

mum possible drop height, but only 0.027 m this time. The last two impacts listed in the table were due to the bag changing conveyors at point O.

Results From Packing Line #2

Test #1:

Test #1 on packing line #2 was run on the section of line between the cross conveyor under the electronic sizer (point A) and the shipping carton packing area (point H). A 6 g threshold was used in this test. A plot of the results can be seen in Figure 3.18 and a listing of the major impacts can be found in Table 3.14.

The first impact listed in Table 3.14 was due to the IS transferring to the bidirectional belt accumulator at point B from the cross conveyor. This impact had the largest maximum possible drop height (0.047 m) in test #1 of line #2. Figure 3.19 shows this impact. The next pair of impacts starting at 252.269 s have unexplained origins with one of the impacts having the highest acceleration level (207 g) recorded in all of the tests.

The next impact at 272.133 s with a 15 g peak occurred while the IS was on the spiral rolls of the bagger. Shortly after the 272.133 s impact, the IS transferred onto the scale pan at point D resulting in two significant impacts. No significant impacts resulted from the IS landing in the bag.

The bag taping operation (bag closing) generated one significant impact along with several low level impacts. The last impact listed in Table 3.14 was caused by the bag of apples being placed in the

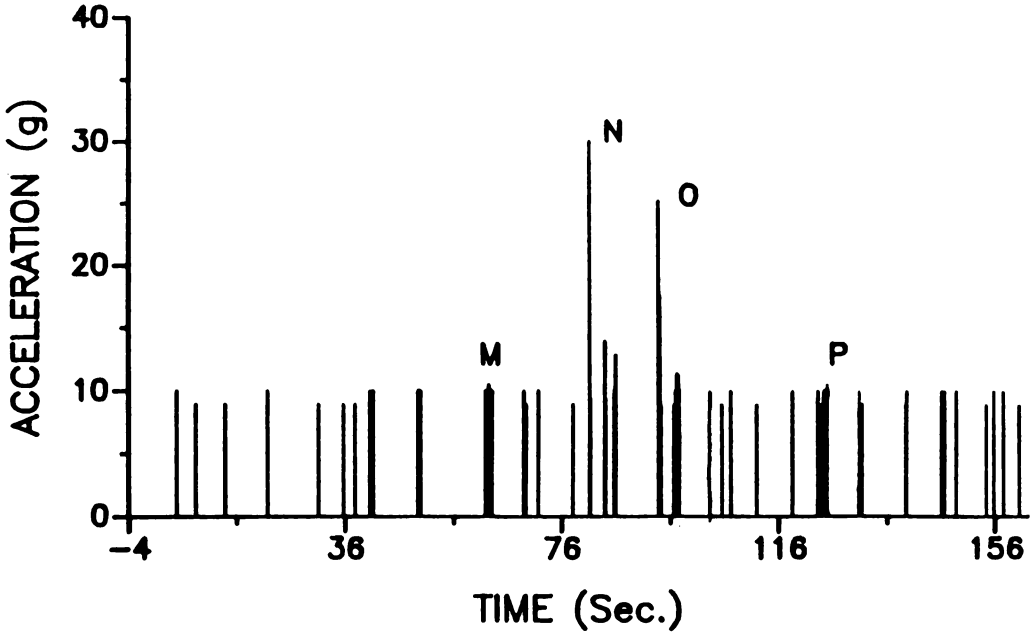

Figure 3.16. Vector sum plot of test #6 on packing line #1 (bagger to shipping carton)

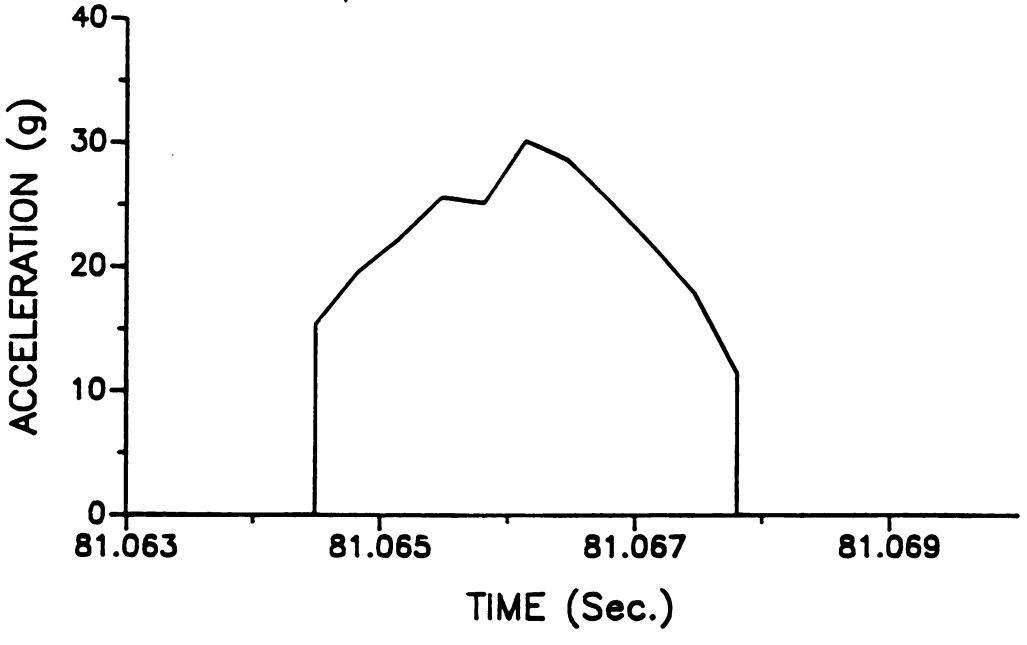

Figure 3.17. .An impact from the bag taping operation at point N.

Table 3.14. Results from test #1 at packing line #2.

Time s	Duration ms	No. Pt #	Peak g	Peak Vel. m/s	MaxDrop m	location
164.151	2.3	7	76.3	0.963	0.047	B
252.269	1.3	4	207.4	0.715	0.026	post B
252.287	1.7	5	13.2	0.156	0.001	post B
272.133	2.3	7	16.9	0.294	0.004	C
273.799	2.0	6	14.8	0.202	0.002	D
273.810	3.3	10	10.9	0.296	0.004	D
301.730	4.6	14	23.8	0.548	0.015	F
351.964	2.3	7	9.7	0.168	0.001	H

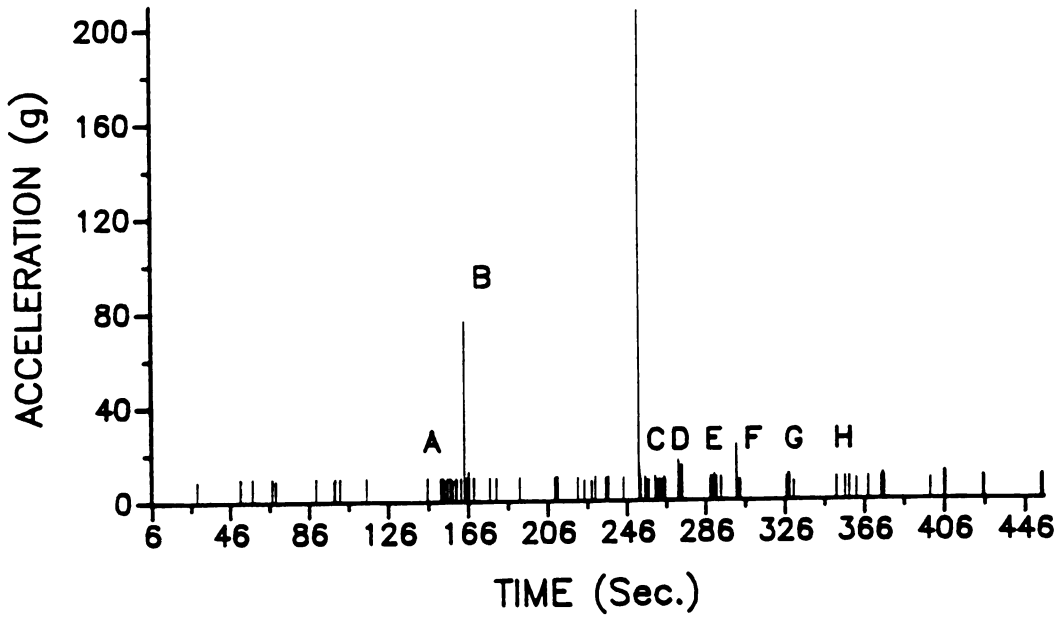

Figure 3.18. A vector sum plot of test #1 on packing line #2.

Table 3.15. Results from test #2 at packing line #2.

Time s	Duration ms	No. Pt #	Peak g	Peak Vel. m/s	MaxDrop m	Location
100.679	3.3	10	73.7	1.309	0.087	B
177.253	4.0	12	23.3	0.635	0.021	post B
229.604	4.6	14	20.3	0.732	0.027	F

shipping carton. It should also be noted that low level impacts were detected from ripping the bag open after the test to retrieve the IS (Figure 3.18).

Test #2:

This test covered the same section of packing line #2 as test #1, however the threshold was set to 8 g. A listing of the major impacts can be seen in Table 3.15.

In this test a 73.7 g impact was recorded when the IS transferred to the bidirectional belt accumulator from the cross conveyor at point B. This impact also produced a maximum possible drop

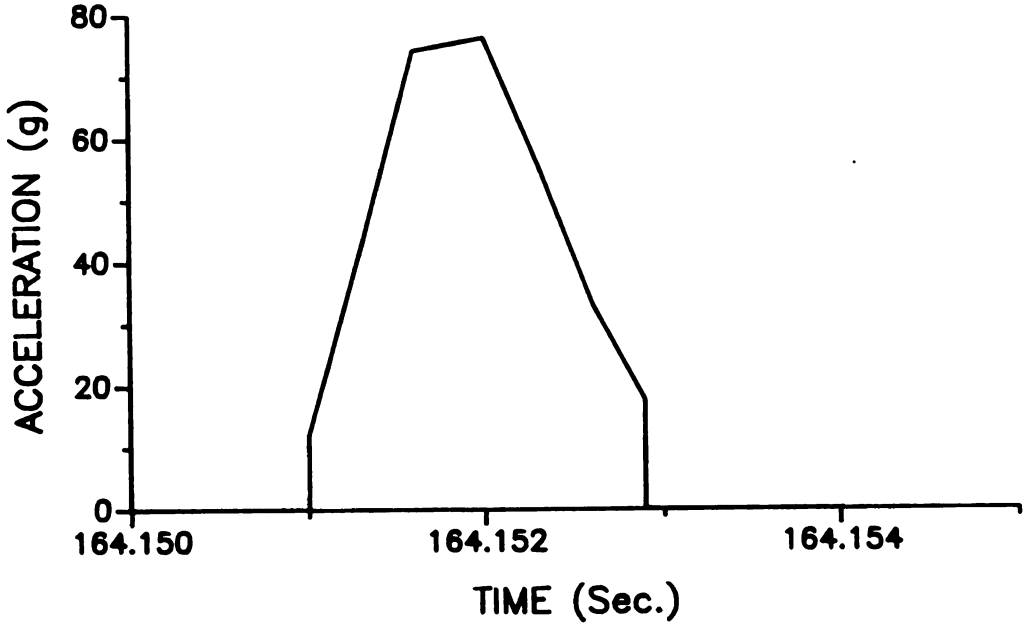

Figure 3.19. An impact from the transfer to the bidirectional belt accumulator at point B on packing line #2.

height of 0.087 m. Another unexplained impact occurred in this test at 177.253 s while the IS was on the bidirectional belts. As in the previous tests, the bag taping operation generated a significant series of impacts.

3.4.3 Discussion

The most interesting phenomena found in both packing lines, were the high levels of acceleration (or impact) encountered in the bag taping operation. It is not known if the impacts were due to the bags hitting the conveyor near the taper or if they were due to the snapping action of the taper.

Both packing lines, on the sections tested, had some problems related to pre-bagging, with the main problem in line #1 being the transfer to the singulater at point F. The impacts seem to be due to the IS and apples rolling past the flap leading to the singulater and hitting the metal dividers. The main problem encountered on line #2 was the transfer to the bidirectional belts at point B which may have been due to the IS hitting the side of the conveyor.

In all of the tests, very few impacts had maximum possible drop heights in excess of 0.01 m with only two impacts reaching 0.1 m. These low maximum drops heights were expected since there were very few free fall drops greater than 0.1 m.

Keeping a good record of events and times while using the IS is important since the IS only records acceleration and real time, but is blind to it's location on the packing line. In the future, even more care should be taken in lining up camera angles and using the built in VCR clock.

The condition, that only data above a give threshold is recorded, causes the loss of detail for low level impacts and causes these impacts to appear square even when they are half sine waves. Low level impacts are also distorted by the the 2 g resolution of the IS. Due to the threshold and the resolution, the IS can only detect the presence of low level impacts (6 or 8 g) but cannot make accurate measurements of them. The fact that most of the low level signals recorded were due to actual impacts and not noise was verified by VCR tapes made at packing line #1. An approximate 2 g positive DC offset before threshold detection appears to be another problem with the measurement of low level impacts. The offset was discovered by noting that most of the low level impacts had only positive values on all three axes.

Another potential problem with the present IS is that it may vibrate at approximately 300 Hz under certain circumstances. This problem was mentioned in the results from test #5 at packing line #1, but low level vibration was also found in some of the other tests. Since the vibrations were noticed on both packing lines and at different locations on the lines, the 300 Hz may be related to the physical properties of the IS.

3.4.4 Conclusions About Packing Line Tests

From the limited numbers of runs made on packing line #1, it appears that the relative problem areas are the transfer to the singulater at point F and the post bagging operations. For the sections of packing line #2 tested, the problem areas appear to be the bag taping operation and the transfer to the bidirectional belt accumulator at point B. It should be noted that the magnitudes of the impacts from a given location often change from run to run. Additional data are required before evaluating the bruising risks to apples.

4. CONCLUSIONS

An impact measurement and analysis system has been developed and successfully tested on an apple packing line. The measurement portion of the system consisted of a microcontroller-based data acquisition unit housed in a 140 mm. diameter sphere. A triaxial accelerometer mounted in the center provides the analog signals. The analysis portion of the system consists of a Pascal program which runs on an IBM or compatible personal computer. The analysis program provides both printed and graphical output. More specifically the conclusions are as follows:

1. The operating system which was developed for the IS performed all of the intended control and communications functions satisfactorily. The operating system contained four top level commands which could be activated from an ASCII terminal. The IS could handle serial communications with software handshaking at five standard baud rates. One of the top level commands was a file transfer routine.
2. The sampling software was capable of sampling three channels at up to 3466 Hz. per channel and conditionally storing the data above a predefined threshold. The sampling period could be changed, through software, by increments of 2.4 μs up to a maximum period of 0.125 s (or 8 Hz.). The times at which the impacts occurred were recorded with a resolution of 614.4 μs. The data for each channel consisted of an 8-bit number which was biased to represent both positive and negative values. This provided a resolution of approximately 2 g (19.6 m/s^2) per digital increment and a range of -256 g to +254 g.
3. The impact analysis software provided an excellent evaluation of the impact data recorded by the IS and provided both tabular and graphical output. During analysis, the following operations are performed on the raw data: scaling, recovery of low frequencies, coordinate rotation, and integration.

The following quantities were also calculated: impact duration, peak acceleration, and total velocity change.

4. From the packing line tests, the IS showed that it was capable of recording all significant impacts encountered in the packing house environment. There was a limitation however on the waveform shape details provided for low level impacts due to the 2 g resolution of the A/D conversion and the thresholding technique used.
5. As a measure of success for this engineering design, it should be noted that the IS operated in a packing line environment without a single software or hardware failure throughout all tests. Battery life also proved to be adequate.

5. FUTURE RESEARCH

Suggestions for future research can be divided into two categories: capturing more information in the recorded data and finding the impact velocity from the acceleration data. As seen in the apple packing line tests in section 3.4, many of the impacts were only 15 g in magnitude while the IS has a resolution of only 2 g which causes a staircase effect when digitizing the impact. However during the same tests a 207 g impact was also recorded which shows a need for a nonlinear coding technique to digitize the impacts. This coding technique could be similar to the IEEE floating point convention which provides a wide range for large numbers and at the same time, high resolution for low magnitude numbers. The CODEC used by Adam et al., as mentioned in section 2.1, may have the desired properties.

Another method of increasing the information available in the recorded data is to record both the leading and trailing impact data. Presently only the data above a set threshold is recorded so that the edges of the acceleration curve are missing. Without the impact edges, it is difficult to characterize low level impacts since the threshold may be set at or near the peak value.

A major limitation in impact analysis has been the lack of knowing the impact velocity. Without the impact velocity it is difficult to determine the energy dissipated during the impact or the maximum deformation of the IS. It should be noted that knowing the energy dissipated during the impact is equivalent to knowing the impact velocity since the total velocity change has been calculated. Energy dissipation can be used to relate impact velocity to rebound velocity by equation [4.1].

$$E_{dissipated} = 1/2\ mv_I^2 - 1/2\ mv_R^2 \qquad [4.1]$$

Fitting the acceleration data to a differential equation which is capable of modeling all the impacts encountered in a packing line appears to be a promising technique for finding the impact velocity.

6. List of References

List of References

1. Adam, V., M. Urbina and R. E. Suarez. 1985. Telemetric Seismic Data-Acquisition System. IEEE Transactions on Instrumentation and Measurement, Vol. IM-34, No. 1, March 1985:81-84.

2. Ahrens, D. A. and S. W. Searcy. 1985. Monitoring Grazing Activities With a Data-Logging System. Agriculutural Engineering, January 1985:18-20.

3. Aldred, W. H. and J. J. Burch. 1977. Telemetry and Microcomputer System Aids Investigation of Forces on Peaches During Mechanical Harvesting. Paper No. 77-1527, Am. Soc. Agr. Eng., 2950 Nile Rd. St. Joseph, MI 49085.

4. Anderson, G. and R. Parks. 1984. The Electronic Potato Departmental Note No. SIN/390, The British Society for Research in Agricultural Engineering.

5. Ball Electronic Systems Division. 1985. Datatrace Preliminary Product Announcement. 9300 West 108th Circle, Westminster, Colorado 80020.

6. Barnes, C. C., J. R. Boddie, J. D. Irwin, G. R. Kane, J. L. Lowry, H. T. Nagle, Jr. and M. H. Willcutt. 1978. Using Finite-State Models in Instrumentation Software. IEEE Transactions on Industrial Electronics and Instrumentaion, Vol. IECI-25, No. 2, May 1978:90-101.

7. Bartram, R.. 1977. Internal Condition (Eating Quality and Appearance of Red and Golden Delicious Apples Found At Retail. Proc. Wash St. Hort. Ass., 73rd. Annual Meeting:88- 92.

8. Chen, P., S. Tang and S. Chen. 1985. Instrument For Testing the Response of Fruits To Impact. ASAE Paper No. 85-3537, ASAE, 2950 Niles Rd., St. Joseph, MI 49085.

9. De Baerdemaeker, J., L. Lemaitre and R. Meire. 1982. Quality Detection By Frequency Spectrum Analysis of the Fruit Impact Force. Trans. ASAE, 25(1): 175-178.

10. Delwiche, M. J.. 1986. Theory of Fruit Firmness Sorting By Impact Forces. ASAE Paper No. 86-3027, Am. Soc. Agr. Eng., 2950 Niles Rd., St. Joseph, MI 49085.

11. Delwiche, M. J. and S. V. Bowers. 1985. Signal Processing of Fruit Impact Forces For Firmness Detection. ASAE Paper No. 85-3029, ASAE, 2950 Niles Rd., St. Joseph, MI 49085.

12. Fluck, R. C. and E. M. Ahmed. 1973. Impact Testing of Fruits and Vegetables. Transactions of the ASAE:660-666.

13. Franke, J. E. and R. P. Rohrbach. 1981. A Nonlinear Impact Model For a Sphere With a Flat Plate. Trans. ASAE, 24(6): 1683-1686.

14. Halderson, J. L., C. L. Peterson and R. C. Daigh. 1983. A Telemetry Device for Impact Detection. Proceedings of the National Conference on Agricultural Electronics Applications, Chicago Dec. 11-13 (2):773-780.

15. Halderson, J. L. and A. Skrobacki. 1986. Dynamic Performance of an Impact Telemetry System. ASAE Paper No. 86-3030, Am. Soc. Agr. Eng., 2950 Niles Rd., St. Joseph, MI 49085.

16. Hamann, D. D. 1970. Analysis of Stress During Impact of Fruit Considered to be Viscoelastic. Trans. ASAE, 13(6):893-900.

17. Hammerle, J. R. and N. N. Mohsenin. 1966. Some Dynamic Aspects Fruit Impacting Hard and Soft Materials. Trans of the ASAE 9(4):484-488.

18. Harrison, D. R.. 1968. FM Telemetry For Multiple Force Measurements On Free-flying Models. Transactions of the IEEE Vol. AES 4(2):194-201.

19. Higuchi, T., T. Saito and A. Kanomata. 1977. A Microprocessor-Based Digital Filter Programmed in a Block Diagram Language. IEEE Transactions on Industurial Electronics and Control Instrumentation, Vol. IECI-24, No. 3, August 1977:231-234.

20. Hill, J. J. and W. E. Alderson. 1981. Design of a Microprocessor-Based Digital Wattmeter. IEEE Transactions on Industrial Electronics and Control Instrumentation, Vol. IECI-28, No. 3, August 1981: 180-184.

21. Horsfield, B. C., R. B. Fridley and L. L. Claypool. 1972. Application of Theory of Elasticity to the Design of Fruit Harvesting and Handling Equipment for Minimum Bruising. Transactions of the ASAE:746-750,753.

22. Intel Corporation. 1986. Microcontroller Handbook. Intel Corporation, 3065 Bowers Ave., Santa Clara, CA.

23. Jenkins, W. H. and E. G. Humphries. 1982. Impact Damage Assessment Technique. Transactions of the ASAE (1982) :54- 57.

24. Klug, B. A., B. R. Tennes, H. R. Zapp, S. Siyami and J. Clemens. 1986. Software for a Miniature Impact Data Acquisition Device. ASAE Paper No. 86-3032, Am. Soc. Agr. Eng., 2950 Nile Rd. St. Joseph, MI 49085.

25. Mattus, G. E.. 1980. Handling and Condition of Apples in Distribution Centers and Retail Stores. Proc. N.Y. State Hort. Soc., 125th. Meeting:160-163.

26. Nahir, D., Z. Schmilovitch and B. Ronen. 1986. Tomato Grading By Force Response. ASAE Paper No. 86-3028, Am. Soc. Agr. Eng., 2950 Niles Rd., St. Joseph, MI 49085.

27. Peleg, K.. 1984. A Mathematical Model of Produce Damage Mechanisms. Transactions of the ASAE: 287-293.

28. O'Brien, M., R. B. Fridley, J. R. Goss and J. F. Schubert. 1973. Telemetry for Investigating Forces on Fruits During Handling. Transactions of the ASAE 16(2): 245-247.

29. Rao, G. P., D. C. Saha, T. M. Rao, K. Aghoramurthy and A. Bhaya. 1982. A Microprocessor-Based System for On-Line Parameter Identification in Continuous Dynamical Systems. IEEE Transactions on Industrial Electonics, Vol. IE-29, No. 3, August 1982: 197-201.

30. Rider, R. C., R. B. Fridley and M. O'Brien. 1973. Elastic Behavior of a Pseudo-Fruit for Determining Bruise Damage to Fruit During Mechanized Handling. Transactions of the ASAE: 241-244.

31. Siyami, S., B. R. Tennes, H. R. Zapp, G. K. Brown, B. Klug and J. Clemens. 1986. Microcontroller Based Data Acquisition System for Impact Measurements. ASAE Paper No. 86-3031, Am. Soc. Agr. Eng., 2950 Nile Rd. St. Joseph, MI 49085.

32. Sridharan, G.. 1984. Microcomputer-Based Synchronous Multichannel Data Acquisition System. IEEE Transactions on Industrial Electronic, Vol. IE-31, No. 4, November 1984: 289-291.

33. Tennes, B. R., H. R. Zapp and G. K. Brown. 1986. Produce Impact Detection and Monitoring Device. ASAE paper No. 86- 3029, Am. Soc. Agr. Eng., 2950 Nile Rd. St. Joseph, MI 49085.

34. Timoshenko, S. P. and J. N. Goodier. 1951. Theory of Elasticity. McGraw-Hill, New York.

35. Wallingford, E. E.. 1982. A Fast, Simple Microcomputer Controlled Data Acquisition System. IEEE Transactions on Instrumentation and Measurement, Vol. IM-31, No. 2, June 1982:137-139.

36. Yang, W. H. 1966. The Contact Problem of Viscoelastic Bodies. J. Appl. Mech. 33:395-401.

37. Zsombor-Morray, P. J., L. J. Vroomen and N. T. Hendriksen. 1981. A Miniature Recording Cardiotachometer. IEEE Transactions on Industrial Electronics and Control Instrumentation, Vol. IECI-28, No. 2, May 1981: 90-97.

7. Appendices

A. Complete Listing For Test #4
At Packing Line #1

Created: 3/ 6/87 11:45:30 a:k04.hex

Time Sec.	Duration msec.	No Pt #	Peak g	VPeak m/s	MaxDrop m
3.416	0.3	1	10.0	0.00000	0.000
8.914	0.3	1	9.0	0.00000	0.000
13.615	0.3	1	10.0	0.00000	0.000
18.372	0.3	1	10.0	0.00000	0.000
27.409	0.3	1	9.0	0.00000	0.000
28.105	0.3	1	10.0	0.00000	0.000
30.101	0.3	1	10.0	0.00000	0.000
32.840	0.3	1	10.0	0.00000	0.000
36.049	0.3	1	10.0	0.00000	0.000
44.722	0.3	1	8.9	0.00000	0.000
49.228	0.3	1	10.0	0.00000	0.000
54.114	0.3	1	10.0	0.00000	0.000
55.268	0.3	1	8.9	0.00000	0.000
58.812	0.3	1	10.0	0.00000	0.000
64.185	0.3	1	9.0	0.00000	0.000
73.043	0.3	1	10.0	0.00000	0.000
101.173	0.3	1	9.0	0.00000	0.000
102.643	0.3	1	10.0	0.00000	0.000
107.449	0.3	1	10.0	0.00000	0.000
109.758	0.3	1	9.0	0.00000	0.000
113.140	3.3	10	14.9	0.39699	0.008
114.006	0.3	1	8.9	0.00000	0.000
114.023	0.3	1	10.0	0.00000	0.000
116.212	0.3	1	8.9	0.00000	0.000
117.291	0.3	1	10.0	0.00000	0.000
128.742	0.3	1	8.9	0.00000	0.000
134.593	0.3	1	10.0	0.00000	0.000
134.799	0.3	1	10.0	0.00000	0.000
134.898	0.3	1	10.0	0.00000	0.000
134.944	0.3	1	11.4	0.00000	0.000
134.958	0.3	1	10.0	0.00000	0.000
134.975	0.3	1	10.0	0.00000	0.000
135.099	0.3	1	10.0	0.00000	0.000
135.106	0.3	1	10.0	0.00000	0.000
135.124	0.3	1	10.0	0.00000	0.000
135.141	0.3	1	10.0	0.00000	0.000
135.162	0.3	1	10.0	0.00000	0.000
135.183	0.3	1	10.0	0.00000	0.000
135.191	0.3	1	10.0	0.00000	0.000
135.198	0.3	1	11.4	0.00000	0.000
135.219	0.3	1	10.0	0.00000	0.000
135.264	0.3	1	10.0	0.00000	0.000
135.268	0.3	1	10.0	0.00000	0.000
135.272	0.3	1	10.0	0.00000	0.000
135.283	0.3	1	10.0	0.00000	0.000
135.286	0.3	1	10.0	0.00000	0.000
135.290	0.3	1	10.0	0.00000	0.000
135.393	0.3	1	10.0	0.00000	0.000
135.492	0.3	1	10.0	0.00000	0.000
135.573	0.3	1	10.0	0.00000	0.000
135.658	0.3	1	10.0	0.00000	0.000
135.887	0.3	1	10.0	0.00000	0.000
135.895	0.3	1	10.0	0.00000	0.000
135.916	0.3	1	10.4	0.00000	0.000
135.919	0.7	2	9.4	0.02964	0.000
135.922	1.3	4	9.4	0.08829	0.000

Created: 3/ 6/87 11:45:30 a:k04.hex

Time Sec.	Duration msec.	No Pt #	Peak g	VPeak m/s	MaxDrop m
135.926	0.3	1	8.9	0.00000	0.000
136.865	0.3	1	9.0	0.00000	0.000
142.345	0.3	1	9.0	0.00000	0.000
142.348	0.3	1	10.0	0.00000	0.000
142.914	0.3	1	10.0	0.00000	0.000
151.341	0.3	1	9.0	0.00000	0.000
155.583	0.3	1	8.9	0.00000	0.000
159.766	0.3	1	8.9	0.00000	0.000
164.068	0.3	1	10.0	0.00000	0.000
165.580	0.3	1	10.0	0.00000	0.000
165.605	0.3	1	10.0	0.00000	0.000
165.957	0.3	1	8.3	0.00000	0.000
169.327	0.3	1	10.0	0.00000	0.000
171.671	0.3	1	8.9	0.00000	0.000
173.793	0.3	1	10.0	0.00000	0.000
176.068	0.3	1	10.0	0.00000	0.000
176.075	0.3	1	8.9	0.00000	0.000
176.124	0.3	1	8.9	0.00000	0.000
178.652	0.3	1	8.9	0.00000	0.000
179.513	0.3	1	10.0	0.00000	0.000
181.939	0.3	1	8.9	0.00000	0.000
181.946	0.3	1	10.0	0.00000	0.000
182.002	0.3	1	8.9	0.00000	0.000
183.562	0.3	1	8.9	0.00000	0.000
183.611	0.3	1	9.0	0.00000	0.000
183.851	0.3	1	10.0	0.00000	0.000
190.161	0.3	1	8.9	0.00000	0.000
190.164	0.3	1	10.0	0.00000	0.000
192.665	0.3	1	8.9	0.00000	0.000
192.936	0.3	1	8.9	0.00000	0.000
192.995	0.3	1	8.9	0.00000	0.000
193.006	0.3	1	8.9	0.00000	0.000
193.454	0.3	1	8.9	0.00000	0.000
197.437	0.3	1	9.0	0.00000	0.000
198.428	0.3	1	9.0	0.00000	0.000
199.812	0.3	1	10.0	0.00000	0.000
199.823	0.3	1	9.0	0.00000	0.000
204.148	0.3	1	8.9	0.00000	0.000
204.406	0.3	1	8.9	0.00000	0.000
206.452	0.3	1	10.0	0.00000	0.000
206.680	0.3	1	9.0	0.00000	0.000
207.368	0.3	1	7.0	0.00000	0.000
211.302	0.7	2	9.0	0.02910	0.000
216.684	0.3	1	8.9	0.00000	0.000
217.694	0.3	1	9.0	0.00000	0.000
218.932	0.3	1	8.9	0.00000	0.000
222.263	0.3	1	10.0	0.00000	0.000
222.280	0.3	1	10.0	0.00000	0.000
222.590	0.3	1	10.0	0.00000	0.000
225.242	0.3	1	9.0	0.00000	0.000
227.969	0.3	1	10.0	0.00000	0.000
229.817	0.3	1	10.0	0.00000	0.000
230.482	3.6	11	15.7	0.43620	0.010
230.525	2.0	6	9.8	0.14400	0.001
230.532	1.0	3	8.9	0.05809	0.000
230.553	1.0	3	9.4	0.05508	0.000

Created: 3/ 6/87 11:45:30 a:k04.hex

Time Sec.	Duration msec.	No Pt #	Peak g	VPeak m/s	MaxDrop m
230.556	1.0	3	9.0	0.05687	0.000
230.560	1.3	4	9.5	0.08595	0.000
230.563	1.3	4	10.8	0.09213	0.000
230.567	1.3	4	10.8	0.10163	0.001
230.571	0.7	2	9.0	0.02885	0.000
230.983	0.3	1	8.9	0.00000	0.000
232.169	0.3	1	9.0	0.00000	0.000
232.228	0.3	1	9.0	0.00000	0.000
233.685	0.3	1	8.9	0.00000	0.000
233.703	0.3	1	8.3	0.00000	0.000
233.755	0.3	1	8.9	0.00000	0.000
233.759	0.3	1	8.3	0.00000	0.000
234.734	0.3	1	9.0	0.00000	0.000
234.742	0.3	1	9.0	0.00000	0.000
235.168	0.3	1	10.0	0.00000	0.000
235.196	0.3	1	8.9	0.00000	0.000
235.332	0.3	1	8.3	0.00000	0.000
235.636	0.3	1	10.0	0.00000	0.000
235.639	0.3	1	10.0	0.00000	0.000
235.674	0.3	1	10.0	0.00000	0.000
235.678	0.3	1	10.0	0.00000	0.000
235.928	1.0	3	9.0	0.05822	0.000
235.932	0.3	1	8.3	0.00000	0.000
236.033	0.3	1	10.0	0.00000	0.000
236.130	0.3	1	10.0	0.00000	0.000
236.141	0.3	1	10.0	0.00000	0.000
236.433	2.0	6	10.7	0.16640	0.001
236.595	0.3	1	8.9	0.00000	0.000
237.406	0.3	1	8.9	0.00000	0.000
242.690	0.3	1	10.0	0.00000	0.000
242.714	0.3	1	10.0	0.00000	0.000
242.806	0.3	1	8.9	0.00000	0.000
242.876	0.3	1	8.9	0.00000	0.000
242.883	0.3	1	8.9	0.00000	0.000
242.896	0.3	1	8.9	0.00000	0.000
243.062	0.7	2	10.5	0.03233	0.000
243.066	0.3	1	10.0	0.00000	0.000
243.158	1.0	3	8.9	0.05809	0.000
243.165	0.7	2	9.0	0.02910	0.000
243.168	0.3	1	8.9	0.00000	0.000
243.412	1.3	4	11.6	0.10457	0.001
243.839	0.3	1	8.9	0.00000	0.000
243.894	0.3	1	8.9	0.00000	0.000
243.950	0.3	1	10.0	0.00000	0.000
244.043	0.3	1	9.0	0.00000	0.000
244.149	0.3	1	9.0	0.00000	0.000
244.325	1.7	5	10.1	0.11186	0.001
244.328	1.3	4	10.2	0.08582	0.000
244.333	0.3	1	10.0	0.00000	0.000
244.335	1.0	3	10.2	0.05577	0.000
244.346	0.3	1	8.9	0.00000	0.000
244.384	0.3	1	8.3	0.00000	0.000
244.391	0.3	1	8.9	0.00000	0.000
244.463	0.3	1	8.9	0.00000	0.000
244.615	1.0	3	9.0	0.05822	0.000
244.621	1.0	3	10.0	0.06469	0.000

Created: 3/ 6/87 11:45:30 a:k04.hex

Time Sec.	Duration msec.	No Pt #	Peak g	VPeak m/s	MaxDrop m
244.626	0.3	1	10.0	0.00000	0.000
244.673	1.0	3	10.0	0.06321	0.000
244.684	0.3	1	10.0	0.00000	0.000
244.701	0.3	1	10.0	0.00000	0.000
244.725	1.0	3	10.4	0.06328	0.000
244.732	1.0	3	10.0	0.06469	0.000
244.736	1.0	3	10.0	0.06501	0.000
244.774	0.3	1	10.0	0.00000	0.000
244.829	1.0	3	10.0	0.06128	0.000
244.833	0.3	1	10.0	0.00000	0.000
244.875	0.3	1	10.0	0.00000	0.000
244.946	3.3	10	12.2	0.31728	0.005
244.954	1.7	5	10.9	0.13940	0.001
245.003	1.0	3	11.3	0.06681	0.000
245.325	1.3	4	10.8	0.10134	0.001
245.334	1.0	3	10.8	0.06666	0.000
245.438	1.3	4	10.6	0.10087	0.001
245.803	0.3	1	10.0	0.00000	0.000
245.855	0.3	1	8.9	0.00000	0.000
245.865	0.3	1	8.9	0.00000	0.000
245.876	0.3	1	10.0	0.00000	0.000
245.879	0.3	1	10.0	0.00000	0.000
245.934	0.3	1	10.0	0.00000	0.000
246.029	0.3	1	9.0	0.00000	0.000
246.031	1.0	3	8.9	0.05517	0.000
246.035	1.0	3	8.9	0.05454	0.000
246.038	1.3	4	9.0	0.08106	0.000
246.042	0.3	1	8.9	0.00000	0.000
246.109	0.3	1	10.0	0.00000	0.000
246.112	0.3	1	8.9	0.00000	0.000
246.116	1.0	3	9.4	0.05889	0.000
246.119	0.7	2	8.9	0.02904	0.000
246.265	0.3	1	9.0	0.00000	0.000
246.339	2.0	6	10.5	0.15255	0.001
246.342	1.7	5	12.1	0.13206	0.001
246.348	2.3	7	12.7	0.21793	0.002
246.356	1.0	3	10.0	0.06128	0.000
246.359	0.3	1	10.0	0.00000	0.000
246.418	2.3	7	14.2	0.24351	0.003
246.426	4.3	13	10.7	0.34289	0.006
246.489	1.0	3	8.9	0.05555	0.000
246.496	0.7	2	8.9	0.02904	0.000
246.499	1.0	3	9.4	0.06129	0.000
246.590	0.3	1	8.9	0.00000	0.000
246.681	0.3	1	10.4	0.00000	0.000
246.684	1.0	3	10.0	0.06128	0.000
246.691	0.3	1	10.0	0.00000	0.000
246.801	3.3	10	12.4	0.32109	0.005
246.805	0.3	1	10.3	0.00000	0.000
247.245	1.7	5	10.8	0.13454	0.001
247.253	2.3	7	12.8	0.21028	0.002
247.411	1.0	3	7.8	0.04898	0.000
247.616	0.3	1	10.0	0.00000	0.000
247.728	0.3	1	8.9	0.00000	0.000
247.731	0.3	1	8.3	0.00000	0.000
247.734	1.0	3	8.1	0.05274	0.000

Created: 3/ 6/87 11:45:30 a:k04.hex

Time Sec.	Duration msec.	No Pt #	Peak g	VPeak m/s	MaxDrop m
247.738	0.3	1	10.2	0.00000	0.000
247.741	0.3	1	9.0	0.00000	0.000
247.797	0.3	1	9.0	0.00000	0.000
247.808	0.3	1	8.9	0.00000	0.000
247.818	0.3	1	10.0	0.00000	0.000
250.327	0.3	1	9.0	0.00000	0.000
250.615	1.3	4	11.7	0.09752	0.000
250.618	1.7	5	10.4	0.12593	0.001
250.622	1.0	3	10.0	0.06128	0.000
250.625	0.7	2	10.0	0.03069	0.000
250.699	0.3	1	8.3	0.00000	0.000
250.838	0.7	2	10.0	0.03256	0.000
250.845	0.3	1	10.0	0.00000	0.000
250.958	3.3	10	12.9	0.33254	0.006
250.994	0.3	1	10.4	0.00000	0.000
251.219	0.3	1	10.3	0.00000	0.000
251.659	0.3	1	9.0	0.00000	0.000
251.708	0.3	1	8.9	0.00000	0.000
253.063	0.3	1	8.9	0.00000	0.000
253.713	0.7	2	9.0	0.02885	0.000
254.430	1.0	3	9.9	0.05611	0.000
254.433	0.3	1	9.5	0.00000	0.000
254.436	1.0	3	8.9	0.05350	0.000
254.441	0.3	1	8.9	0.00000	0.000
254.503	0.3	1	8.3	0.00000	0.000
254.677	1.0	3	9.4	0.05929	0.000
254.681	0.7	2	8.9	0.02904	0.000
254.685	1.7	5	10.8	0.12156	0.001
254.688	0.3	1	9.0	0.00000	0.000
254.731	0.3	1	9.0	0.00000	0.000
254.783	0.3	1	10.0	0.00000	0.000
254.867	0.3	1	8.9	0.00000	0.000
254.947	0.3	1	10.0	0.00000	0.000
255.011	0.3	1	10.3	0.00000	0.000
255.062	0.7	2	10.4	0.03215	0.000
255.367	1.3	4	10.9	0.10260	0.001
255.512	1.3	4	10.9	0.10006	0.001
255.518	2.3	7	10.9	0.20253	0.002
255.576	0.3	1	10.1	0.00000	0.000
255.749	0.3	1	8.9	0.00000	0.000
255.774	0.3	1	9.0	0.00000	0.000
255.902	0.3	1	8.9	0.00000	0.000
256.320	0.3	1	8.9	0.00000	0.000
256.323	0.3	1	9.0	0.00000	0.000
256.410	0.3	1	8.9	0.00000	0.000
256.637	1.0	3	8.4	0.05330	0.000
256.640	0.7	2	8.3	0.02636	0.000
256.643	0.3	1	8.9	0.00000	0.000
256.703	1.0	3	8.3	0.05373	0.000
256.707	1.0	3	8.9	0.05809	0.000
256.710	1.0	3	8.9	0.05809	0.000
256.748	0.3	1	8.3	0.00000	0.000
256.762	0.3	1	9.0	0.00000	0.000
256.766	0.3	1	8.9	0.00000	0.000
256.769	0.3	1	8.9	0.00000	0.000
257.010	0.3	1	9.8	0.00000	0.000

Created: 3/ 6/87 11:45:30 a:k04.hex

Time Sec.	Duration msec.	No Pt #	Peak g	VPeak m/s	MaxDrop m
257.014	0.3	1	8.8	0.00000	0.000
257.017	0.3	1	9.8	0.00000	0.000
261.759	0.3	1	8.9	0.00000	0.000
267.865	0.3	1	10.0	0.00000	0.000
267.900	0.3	1	10.0	0.00000	0.000
270.612	0.3	1	10.0	0.00000	0.000
275.140	0.3	1	10.0	0.00000	0.000
275.492	0.3	1	8.9	0.00000	0.000
283.661	0.3	1	8.9	0.00000	0.000
291.134	0.3	1	10.0	0.00000	0.000
301.024	0.3	1	11.4	0.00000	0.000
301.027	0.3	1	10.5	0.00000	0.000
301.034	0.3	1	11.8	0.00000	0.000
301.037	0.3	1	10.0	0.00000	0.000
301.041	0.7	2	11.4	0.03465	0.000
301.044	0.3	1	11.4	0.00000	0.000
301.048	0.7	2	10.0	0.03256	0.000
301.051	0.3	1	11.8	0.00000	0.000
301.055	0.3	1	11.4	0.00000	0.000
301.058	0.3	1	11.8	0.00000	0.000
301.061	0.3	1	11.4	0.00000	0.000
301.065	0.3	1	11.4	0.00000	0.000
301.068	0.3	1	10.0	0.00000	0.000
301.072	0.7	2	10.0	0.03256	0.000
301.075	0.3	1	10.0	0.00000	0.000
301.078	0.3	1	10.0	0.00000	0.000
301.082	1.0	3	10.0	0.06513	0.000
301.085	0.3	1	11.8	0.00000	0.000
301.089	0.3	1	10.0	0.00000	0.000
301.092	0.7	2	10.5	0.03315	0.000
301.096	0.3	1	10.5	0.00000	0.000
301.099	0.3	1	10.0	0.00000	0.000
301.106	0.3	1	11.4	0.00000	0.000
301.120	0.3	1	10.5	0.00000	0.000
301.130	0.7	2	10.0	0.03256	0.000
301.151	0.3	1	10.0	0.00000	0.000
301.161	0.3	1	10.0	0.00000	0.000
301.165	0.3	1	10.0	0.00000	0.000
301.175	0.3	1	10.0	0.00000	0.000
301.179	0.3	1	10.0	0.00000	0.000
301.188	0.3	1	11.4	0.00000	0.000
301.199	0.3	1	10.0	0.00000	0.000
301.206	0.3	1	11.4	0.00000	0.000
301.217	0.7	2	10.0	0.03256	0.000
301.220	0.3	1	10.0	0.00000	0.000
301.223	0.3	1	10.0	0.00000	0.000
301.227	0.3	1	10.0	0.00000	0.000
301.234	0.3	1	10.0	0.00000	0.000
301.244	0.3	1	10.0	0.00000	0.000
301.251	0.3	1	10.0	0.00000	0.000
301.254	0.3	1	10.0	0.00000	0.000
301.262	0.3	1	10.0	0.00000	0.000
301.710	0.3	1	10.0	0.00000	0.000
306.652	0.3	1	10.0	0.00000	0.000

B. IS Operator Handbook

The purpose of this handbook is to acquaint the reader with the operation of the Inst Sphere (IS) when used with an IBM or compatible personal computer. The following assump be made about the personal computer: a virtual disk (RAM disk) is setup upon booting, the has two floppy disk drives, the computer has been booted before starting, and the IS progra placed in drive "A". In the rest of this handbook, keyboard control keys or combinations of co will be enclosed in the following brackets: "< >".

1. Installation of Software

At minimum the following files must be present on the program disk:

```
TESTSYS.EXE
ERROR.MSG
4X6.FON
KERMIT.EXE
MSKERMIT.INI
BALL.CAL
TESTSYS.CFG
COMM.BAT
GRAPHICS.COM
```

It is also possible to run the IS software from a hard drive.

After copying all of the above files onto a disk, TESTSYS.CFG should be edited with editor to make sure that the virtual disk designator on the first line of the file is correct.

2. Connecting Hardware

The first step is to plug the IS interface box (the interface box is a 130x100x70 mm. b into a 120 VAC outlet; all of the switches should be in the off position. The IS interface cabl ing a DB9 connector and a 5 pin round connector should be connected next. The end cont

B. IS Operator Handbok

DB9 is plugged into the interface box while the 5 pin connector is plugged into the IS. The final connection is made between the DB25 on the IS interface box and COM1 on the personal computer.

3. Start-Up

The first step in start-up is to invoke the terminal emulator KERMIT on the personal computer. After placing the IS program disk into drive A, enter the following from the keyboard:

```
A: <Cr>
COMM <Cr>
C <Cr>
```

The power switch on the interface box should now be turned on. In order to charge the batteries, the red charging button on the interface box should now be pressed to put the IS in the heavy charge mode; heavy charge will be indicated by a red LED. Then the switch labeled "IS OFF-ON" should be turned to the "on" position. Upon turning on the last switch, the following message should appear on the screen:

```
INSTRUMENTED SPHERE      PROTOTYPE
MICHIGAN STATE UNIVERSITY
ALL RIGHTS RESERVED
PATENT PENDING
```

At this time any of the following commands may be entered from the keyboard: RDATA, SEND, DISPLAY, and BAUD.

4. Starting Data Collection

Before continuing, the "Caps Lock" key on the keyboard should be pressed. In order to collect data at 3000 Hz. with a 10 g threshold at 1:00 pm on May 20, 1987, the following should be entered from the keyboard:

```
RDATA <Cr>
P <Cr>
3000 <Cr>
10 <Cr>
G <Cr>
05/20/87 <Cr>
```

```
13:00:00 <Cr>
E <Cr>
```

5. Collecting Data

After data collection has been started, the 5 pin connector may be unplugged from the IS. All of the switches on the interface box should be left in the "on" position. Since the IS is now unplugged, it may be run through a packing line or impacted in some other manner. After recording impact data, the IS should be brought back to the interface box and the 5 pin connector reconnected.

6. Stopping Data Collection

Data collection is stopped by entering the following from the keyboard:

```
RDATA <Cr>
Q <Cr>
E <Cr>
```

7. Up-Loading the Data to the Personal Computer

The IS data is up-loaded to the personal computer by entering the following from the keyboard:

```
SEND <Cr>
<Ctrl-]> C
LOG filename <Cr>
C <Cr>
<Cr>
```

At this point data should be flowing to the personal computer. After data stops scrolling across the screen, the following should be entered from the keyboard:

```
<Ctrl-]> C
CLOSE <Cr>
```

If no further tests are to be made with the IS, KERMIT should be exited by entering "E <Cr>".

8. Start Up of the Analysis Software (TESTSYS)

Upon exiting KERMIT you should be at the DOS command level and the analysis software may by started by entering the following:

```
GRAPHICS <Cr>
TESTSYS <Cr>
```

TESTSYS will write the following to the screen:

```
TESTSYS PROGRAM  BY B. KLUG  1987
VERSION 1.02

I- INPUT A HEX DATA FILE
C- IS DATA ANALYSIS
L- LIST ANALYSIS RESULTS
P- PLOT DATA
D- DISPLAY DATABASE
A- AUXILIARY MENU E- EXIT TESTSYS

ENTER DESIRED COMMAND  >
```

In order to input an IS data file, enter the following:

```
I <Cr>
filename <Cr>
BALL.CAL <Cr>
```

9. Running an Analysis on the IS Data

After the IS data file has been read, a complete analysis may be run by entering "C <Cr>" from the keyboard.

10. Listing the Analysis Results

The results from the analysis may be listed on the screen by the following commands:

```
L <Cr>
CON <Cr>
Y <Cr>
```

If you want the results printed, replace "CON" with "PRN" in the above sequence.

11. Plotting the Impact Data

The vector sum of the impact data may be plotted on the screen by entering the following from the keyboard while at the TESTSYS command level:

```
P <Cr>
S <Cr>
<Cr> N <Cr>
<Cr>
V <Cr>
```

After entering the above sequence, a plot should appear on the screen. This plot may be printed by typing "<Shift-PrtSc>". Any other key will erase the plot.

12. Storing the IS

When the IS is not in use, the IS OFF-ON switch on the interface box should be turned to the "off" position. The power switch on the interface box may be left on for trickle charging. However if the IS is not going to be used in the near future, the power switch should be turned off and the box should be disconnected from the IS. During storage, a dummy plug should also be inserted into the IS.